Progress in Aerospace Sciences 152 (2025) 100900

Contents lists available at ScienceDirect

Progress in Aerospace Sciences

journal homepage: www.elsevier.com/locate/paerosci

Recent innovations to advance space electric propulsion technologies

Igor Levchenko [a,*], Dan Goebel [b,**], Daniela Pedrini [c], Riccardo Albertoni [d], Oleg Baranov [e,f], Igal Kronhaus [g], Dan Lev [h], Mitchell L.R. Walker [h], Shuyan Xu [a,***], Kateryna Bazaka [i,****]

[a] Plasma Sources and Application Centre / Space Propulsion Centre Singapore, Nanyang Technological University, 637616, Singapore
[b] NASA Jet Propulsion Laboratory, California Institute of Technology, Pasadena, CA, 91101, USA
[c] SITAEL Space Division, Pisa, 56121, Italy
[d] Airbus Defence & Space, Toulouse, France
[e] National Aerospace University, Kharkiv, Ukraine
[f] Jožef Stefan Institute, Ljubljana, Republic of Slovenia
[g] Technion - Israel Institute of Technology, Space Plasma Technologies, Inc., Haifa, Israel
[h] School of Aerospace Engineering, Georgia Institute of Technology, Atlanta, GA, 30332-0150, USA
[i] School of Engineering, The Australian National University, Canberra, ACT 2601, Australia

ABSTRACT

While many types of mature space propulsion systems are in active use, significant progress is still required to meet the requirements of new missions. The emerging challenges include plans for Mars and Moon exploration, building huge satellite constellations like Starlink and OneWeb, advanced astrophysical studies including space-based gravitational wave detection systems, precise astrophysical and astronomical measurements in space, search for life on exoplanets, deep space missions, and others. In this light, this review outlines and briefly discusses the most recent, advanced and innovative approaches, technologies, concepts, and physical principles related to space propulsion. Furthermore, we present more ambitious ideas for the future that have been demonstrated in labs as prototype space systems to enhance the performance of mature space propulsion thrusters and concepts that are proposed for consideration in future space thruster systems. We discuss the recent advances in the application of advanced rotating magnetic field systems for space propulsion, condensable propellant thrusters, innovations in propellant supply systems, capillary and narrow channel thrusters, staged thrusters, application of segmented electrodes, and other techniques. The manuscript brings to light the most recent innovations for future consolidated research efforts worldwide, helps to define the key parameters of space propulsion systems for future ambitious missions, and ultimately contributes to the creation of substantially novel thrust platforms for future space exploration.

1. Introduction

We stand witness to the birth of a new space era: space tourism has become a reality, constellations of satellites have become an enabling platform for ambitious projects that touch virtually every facet of our life on Earth, and sufficient technological progress has been achieved to enable the exploration and colonization of Moon and Mars [1–3]. The space sector is destined to become a major driver and enabler for the economy of the future, as companies and governments allocate huge investments to space technology, and all space-related activities have a wide resonance on social media. The advances in microelectronics and miniaturized systems allowed space assets to become smaller [4], creating a vibrant and rapidly growing micro- and mini-satellite markets [5–7]. Given the primary role advanced space propulsion plays in this context, researchers in the field focus on devising new concepts for creating thrust in space [8,9], and on efficiently implementing the existing thruster systems [10,11]. Space systems that utilize plasma [12–15] and ionized gas [16–18] to create thrust are particularly appealing due to many advantages [19–21], mainly related to very high specific impulse [22–24] and potentially long service life [25,26]. Advanced applications of plasma systems can stimulate new research directions, ranging from space debris removal to maintenance and repair operations in open space [27].

There are still several challenges in the further development of the

* Corresponding authors.
** Corresponding author.
*** Corresponding authors.
**** Corresponding author. School of Engineering, The Australian National University ACT 2601, Canberra, Australia.
E-mail addresses: I.Levchenko@post.com (I. Levchenko), dan.m.goebel@jpl.nasa.gov (D. Goebel), mitchell.walker@ae.gatech.edu (M.L.R. Walker), Shuyan.Xu@nie.edu.sg (S. Xu), katia.bazaka@anu.edu.au (K. Bazaka).

https://doi.org/10.1016/j.paerosci.2023.100900
Received 30 September 2022; Received in revised form 20 March 2023; Accepted 22 March 2023
Available online 16 December 2024
0376-0421/

existing advanced propulsion systems. Firstly, an increase in specific impulse is needed to enable all the potential applications of electric and plasma propulsion systems, ranging from small satellites to large, manned spacecraft directed toward the Moon and Mars. Secondly, work must be done to extend the lifetime of plasma thrusters, which is still insufficient to complete many demanding missions (e.g., investigation of remote planets and deep space exploration). Finally, a significant endeavor shall be dedicated to the improvement of the cathode, a critical part of plasma thrusters and that affects the total efficiency, reliability, and lifetime of the entire propulsion system.

The innovations in the present space propulsion technologies include enhancing the plasma control in the electric propulsion (EP) thrusters, introduction of new control mechanisms, the utilization of alternative propellants to xenon, to address the requirements of the recently emerged missions. On the other hand, many different concepts exist whose maturity is still low yet they are promising for the creation of novel thrust platforms. Alternative propulsion systems are explored with the aim of making space vehicles greener, faster, more reliable, cheaper, and more durable. In some cases, innovative solutions are mandatory to reach new goals; for example, light-enabled space propulsion is one of the few currently known realistic options for future interstellar travels. The same physical principle, e.g., using light or magnetic reconnection to create thrust, can be exploited in many ways and implemented in different devices, as described later in this Review. Emerging technologies are prone to a shorter time to market, due to low-cost and rapid methods of developing and testing made possible by the progress in diagnostics.

Since no single propulsion technology is suitable for the entire variety of space missions, a diversity of propulsion solutions should be maintained and brought to an advanced readiness level to fulfill a diverse set of functions. The requirements for in-space propulsion broadly vary according to the intended application. The possibility of implementing multimode systems, *i.e.*, propulsion systems with two or more modes achieved with a single propellant, could allow for a high level of adaptability and flexibility [28]. Concepts combining monopropellant, bipropellant, and solid chemical propulsion with electrothermal, electrostatic, and electromagnetic EP have been or are being investigated. In general, for a given mission, a tradeoff is sought between multiple parameters, namely efficiency, thrust, specific impulse, compactness, and thrust-to-power ratio. Manufacturability and cost are also primary aspects to consider. The researchers share a common endeavor for improvements in transit times, payload mass, safety, reliability, and durability of propulsion systems. As very important recent missions, the successful mission to asteroid Bennu, NASA's OSIRIS-REx asteroid-sampling mission [29–31], and the successful return of samples from Ryugu could be mentioned here [32,33]. Space exploration assets have become essentially electrical and very diversified in physical principles. Thus, new ideas, concepts, and perspective technologies should be examined [34,35].

While many types of space EP systems are mature and active in space, significant progress is still required to address the new tasks and challenges that emerged recently, such as plans for Mars and Moon exploration [3,36], building huge satellite constellations [37] such as Starlink and OneWeb [38–40], advanced astrophysical studies including space-based gravitational wave detection systems [41–44], precise astrophysical and astronomical measurements in space [45–47], search for life on exoplanets [48], and others. From this perspective, we aim this review to examine the most recent, most advanced aspects and physical principles that will help enable the following [49–51].

- ✓ *To ensure a breakthrough in the extending of the operation life of mature EP systems for long two-way journeys to/from Mars, as well as for remote planet exploration;*
- ✓ *To enhance the efficiency of the thrusters via innovative, not yet explored physical principles and technological approaches that were recently demonstrated in labs or* conceptualised *for the application in space propulsion systems;*
- ✓ *To ensure ultra-precise position and attitude control for special astrophysical missions such as drag-free flight in the gravitational wave detection systems in space, space-based measurement systems, geodesy, fundamental physics measurements, and space-based platforms for fundamental physics studies.*

The general aim of this review is to outline and help define the most relevant innovations for the future consolidated research efforts, and to finally help to enhance the key parameters of space propulsion systems for the ambitions future missions such as Mars and Moon exploration, investigation of remote planets, and supporting the deep space missions.

2. Electric space propulsion today – a brief overview

While the survey and even the brief outline of the existing, mature space propulsion systems is *well outside the scope of our review*, here we list and briefly characterize the key types of space propulsion thrusters, with a view to highlight the whole spectrum of these systems and help the general physical audience to orient themselves in the flourishing diversity of the existing space propulsion systems [5,7,11].

According to the *ideal rocket equation*, the velocity increment attained by a space vehicle is $\Delta v = Ve \ln (Mi/Mf)$, where $\dot{m}$ is the rate of variation of the vehicle mass (kg/s), ***Ve*** is the effective exhaust velocity (m/s), and *Mi* and *Mf* are the initial and final mass of the spacecraft, respectively [52]. Since the velocity increment is linearly dependent on the effective exhaust velocity ***Ve***, this value should be as high as possible. While in the case of chemical propulsion *the highest* ***Ve*** is indeed the ultimate aim, it is not always desired for EP systems since the EP systems create thrust by accelerating plasma and ions, and the *thrust-to-power ratio* is also a very important characteristic which strongly depends on the mission requirements, type and power of the on-board power supply system, and many other considerations [53].

EP systems span five orders of magnitude in power, and two orders of magnitude in the specific impulse (Fig. 1). Such considerable diversity enables the use of this family of thrusters across very different missions, from the smallest cubesat systems to large, powerful spacecraft designed for, e.g., manned flights to Mars. Insets illustrate the principal schematics of each device type. Note that the colored ovals marking the power/specific impulse zones are tentative, to sketch these key parameters by order of magnitude and to illustrate how various types of thrusters can complement each other and for different missions. For more specific numbers and other important parameters of various types of thrusters the reader could refer to the fundamental monographs [52,54] and recent comprehensive review papers [5,7,10,19,20,24,28,34].

1. ***Vacuum arc thrusters*** utilize a discharge between two electrodes (most often, in the coaxial configuration yet flat geometry is also possible). The cathode is eroded in localized regions known as cathodic spots, where the discharge is attached to the surface. Metal plasma emitted from these micrometer-sized spots is accelerated via gas-dynamic expansion and ponderomotive forces originated from the interaction of magnetic field with electric current. Those thrusters feature low-to-medium specific impulse.
2. ***Pulsed thrusters*** work similarly to magnetically enhanced vacuum arc thrusters but in a pulsing mode. They produce medium impulses and a higher level of power, due to their pulsing character that allows cooling between pulses and their design allows to cope with potential energy limitations.
3. ***Electrospray (colloid) thrusters*** electrostatically accelerate the charged droplets of liquid to create thrust. In the thrusters of this type, the charged droplets are created via electrospray process. Electrons are injected into the jet of droplets via a cathode-neutralizer (which can be seen in Fig. 1 above as a thin tube atop the thruster body).

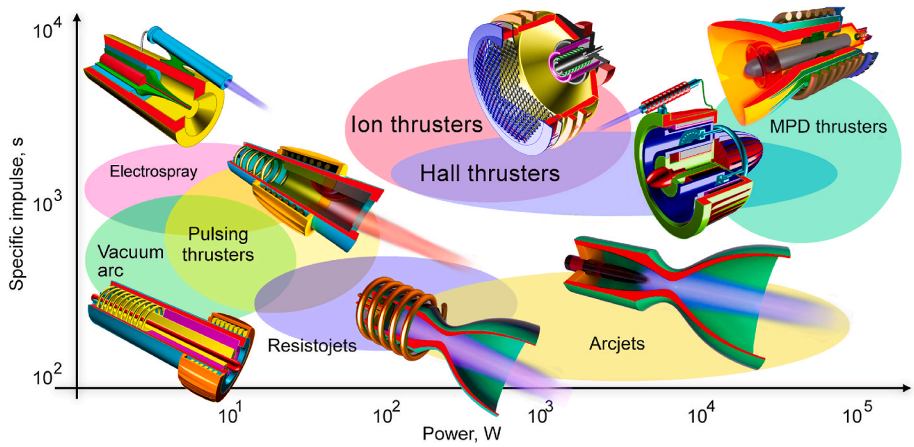

Fig. 1. Main types of space electric propulsion systems in the power – specific impulse coordinates. Very wide power and specific impulse ranges allow the application of EP on quite various missions and spacecraft, ranging from small CubeSats to large systems for the human transportation to Moon and Mars. To enhance the performance of existing EP systems, prolong their operational life and enhance the reliability, further advanced ideas and concepts should be explored and some of them are discussed in this review. Note that the colored ovals marking the power/specific impulse zones are tentative, to sketch these key parameters by order of magnitude and to illustrate how various types of thrusters can complement each other and be used for different missions. For more specific numbers and other important parameters the reader could refer to the fundamental monographs and recent comprehensive review papers.

4. ***Resistojet thrusters*** utilize a heating of non-reactive fluids by an electric current flowing via incandescent heating elements. The high-temperature gas is then expanded in the nozzle and generates thrust.
5. ***Ion thrusters*** utilize the neutral gas, which is then ionized in the discharge chamber. The ions are then accelerated by an electrostatic field, while electrons are injected into the ion jet via a cathode.
6. ***Hall thrusters*** use the Hall effect (by Edwin Hall) in the radial magnetic field and axial electrostatic field. This ensures efficient ionization of the propellant and acceleration of ions to generate thrust. Electrons are also injected into the plasma beam via a cathode, which can be observed in Fig. 1 as a thin tube atop the thruster body.
7. ***Arcjets*** use an electrical discharge (arc) in gas-phase propellants such as hydrazine or ammonia, to bring additional energy to the propellant and thus increase the exhaust velocity due to additional energy consumed by the propellant. The arcjets could physically operate in a very wide power range, spanning from 10^2 to 10^5 W yet the materials-related problems make the very high powers problematic.
8. ***Magnetoplasmadynamic (MPD) thrusters*** use a gaseous material that is fed into an acceleration chamber and then ionized. The ions are then accelerated via Lorentz force which is created from the interaction of the electric current in plasma, and the magnetic field. It can feature very high power and specific impulse, yet at the expense of a very high energy cost (Watt per Newton) of the thrust. It should be noted that this type of thrusters is sub-divided to the three major groups, namely the self-field, self-field with low applied magnetic fields, and applied-field thrusters. While the self-field systems rely on the magnetic field produced by the discharge current, the applied-field thrusters use external coils that are powered by additional power supply units and produce the magnetic field to realize the acceleration of plasma. Apparently, the external coils could incorporate many turns and thus can produce the required levels of magnetic field by relatively low current, much lower than the discharge current. The self-field thrusters with low applied magnetic field is the system where a weak diverging magnetic field is applied in the anode/nozzle region to damp instabilities and what is called "onset" (which is a high oscillation mode characterized by anode sputtering and damage). Onset limits the discharge current, power and performance. The low applied field does not contribute significantly to the electromagnetic thrust, but helps to raise the discharge current significantly, up to two-hold. As a results, a power level of MW is achievable for the applied-field thrusters [55]. Various power levels are also reported, e.g. 100 kW [56], 200 kW, 400 kW [57] thus making this type of thrusters quite promising for the future missions [58,59].

The vast diversity of power, efficiency, schematics, size, and thrust levels makes it possible to find the most matching solutions among the EP platform for virtually any type of spacecraft, from CubeSats to huge Earth-Mars transportation systems.

It should be noted that among the diversity of the above-mentioned parameters and characteristics, the propellant flexibility and thruster throttability are also important to easily and efficiently adapt the thrusters to various missions by changing the propellant and thrust without significant re-designing of the flight tested units. Not surprisingly, a series of multi-propellant thrusters has recently been developed and successfully tested, e.g. Hall type thrusters capable of working on Xenon and Krypton (as Krypton is significantly cheaper than traditionally used Xe) [60,61]. In view of the importance of this feature, we will discuss below the progress in this field in more detail.

Table 1 lists several recently reported characteristics of various types of EP thrusters, to present the currently achieved levels of efficiency and a wide range of thruster power levels, ranging from several W to tens of kW.

Note that the electrodeless thrusters form a somewhat separate group of electric propulsion systems and would require a separate graphical diagram to illustrate their characteristics. More detailed information on specific physical mechanisms, principles of operation, characteristic parameters, advances and disadvantages of various electrode-utilizing and electrodeless thrusters of various types could be found in the comprehensive reviews and original publications cited herein [5,7,8,10,14,19,20,24,28,34,81–83].

3. Active plasma control in electric thruster systems

Active plasma control is important for virtually all types of thrusters, including micro-cathode thrusters which are very simple in their design, consisting mainly of the cathode and axial anode, sometimes fitted with an auxiliary magnetic coil. They ensure relatively high specific impulse and are widely used for the attitude control systems of small satellites [84,85]. Importantly, they could be made to be very small, and suitable for application at Cubesats and ultra-small satellites. On the other hand, their specific impulse should be enhanced to ensure long, for several years, in-orbit active control. This aim could be achieved in two ways,

Table 1
List of recently published characteristics of several key types of EP thrusters.

Thruster	Year	Status	Power	Thrust	Isp, sec	Efficiency	Ref.
Hall thrusters							
PPS-X00	2020	Development	200–1000 W	43 mN (@650W)	1,530 (@650W)	0.4	[62,63]
H-9 (Xe & Kr)	2021	Lab	4.5–9 kW	295–450 mN (Xe) 240–350 mN (Kr)	1,900–2,780 (Xe) 1,900–2,700 (Kr)	0.64–0.73 (Xe) 0.52–0.54 (Kr)	[64]
HT20K	2021	Lab	6–19 kW	400–910 mN (Xe)	–	–	[65]
Wall-less low power HET	2021	Lab	190–370 W	5–11.5 mN (Xe)	1,020–1,200 (Xe)	0.135–0.19	[66]
MASMI	2021	Qualification	200-1,000 W	14–68 mN (Xe)	900-1,900 (Xe)	0.25–0.51	[67]
100-kW nested HET	2021	Lab	5–102 kW	<5 4. N (Xe)	1,800–2,650 (Xe)	0.54–0.67	[68]
300W HET	2022	Lab	150–500 W (Xe) 250–450 W (Kr)	9–22 mN (Xe) 11–18 mN (Kr)	850-2,000 (Xe) 1,100–1,700 (Kr)	0.28–0.44 (Xe) 0.26–0.34 (Kr)	[69]
Steady-state applied-field MPD thrusters							
CAS	2018	Lab	150 kW	–	5,600 (Ar)	0.76	[70,71]
SX3	2019	Lab	150 kW	0.4–3.59 N	<4,665 (Ar)	0.2–0.62	[55]
AF-LFA	2018	Lab	30 kW	0.111 N	–	–	[72]
Gridded ion thrusters							
Gridded ion thruster	2022	Lab	200 W	40 mN (Estim.)	–	0.6–0.75 (Xe, I, Ar, Kr)	[73]
GIESEPP (T5) GIESEPP (T6)	2022	Lab	215–4058 W 1704–32,221 W	23.7 mN 145 mN	1434–2711 1845 - 34,885	0.86	[74,75]
IonJet	2022	Lab	6–14 W	0.8–1.56 mN	<1000	–	[76]
Other types of thrusters							
Helicon HIPATIA thruster	2022	Lab	200–450 W	2.5–6.5 mN	400 s	0.5	[77–79]
IFM Nano Thruster	2022	Lab	50 W (beam)	475 mN	4500 s	30%	[80]

mainly by influencing plasma acceleration in the discharge and through the active control of the plasma after discharge.

3.1. Additional magnetic coils and electrodes

Application of *additional magnetic coils and additional electrodes* to intensify the discharge and control the exhausting plasma is a natural way to enhance the parameters of the thruster. The influence of the magnetic field on the discharge parameters has a complex character (Fig. 2). The influence of the magnetic field on the energy of ions generated in a cathodic spot is described by a non-monotonic dependence, when the energy is increased as the magnetic field increases from zero values, and then reaches a saturation mode [86]. Both the electron temperature and kinetic energy of ions are affected by the magnetic field of less than 0.05 T at the arc discharge current of about 500 A; this trend is observed for cathodes made of titanium, carbon, and uranium [87]. Furthermore, the presence of the magnetic field B does not change the shape of the distribution of electron energy, since it stays Maxwellian, but increases the average energy of electrons ε_e from about $\varepsilon_0 \approx 1$ eV for zero magnetic field and 5–10 eV for the magnetic fields less than 0.05 T. The trend is stable for various cathode materials. The observed dependence is described well by the relation: $\varepsilon_e(B) = \varepsilon_{e0} + \alpha_{\varepsilon B}\sqrt{B}$.

It should be mentioned that in the case of very strong magnetic fields (typical for e.g. magnetic nozzles, see sub-section 3.5 below), the processes are more complicated. Details can be found in the dedicated reviews e.g. Ref. [89] and in the recent original research publications [90–94].

3.2. Segmented electrodes and other techniques

Segmentation of electrodes has always been a viable method to assess, investigate and implement systematic analyses on the level of voltage and current variations, thrust and life time-related issues referring to the electrodes. An example is the first stage of the hybrid thruster

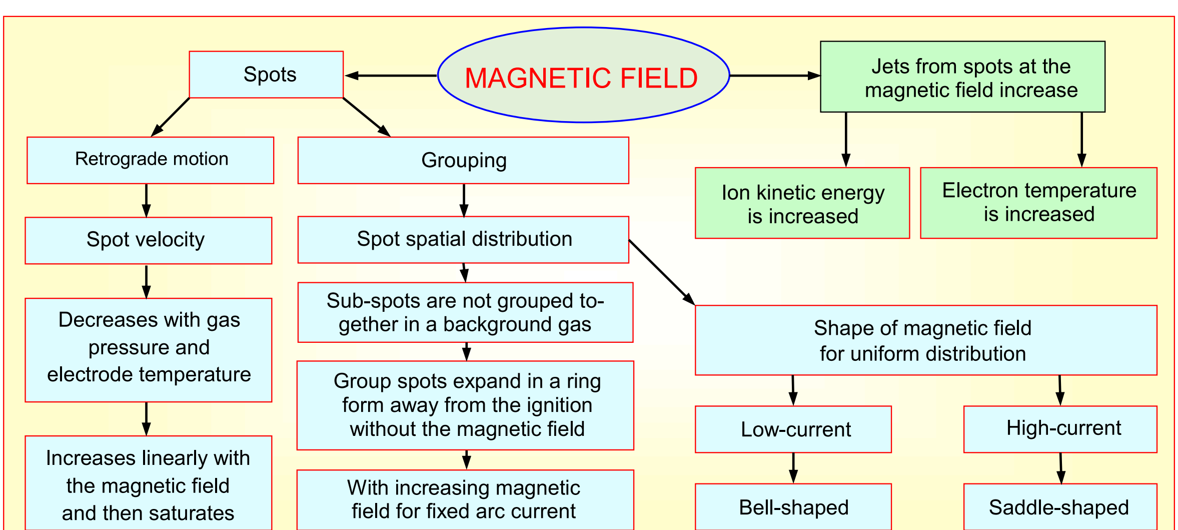

Fig. 2. Influence of the magnetic field on arc parameters. The magnetic field resulted in (1) increased charge states, (2) increased average ion energies approximately proportional to the charge state, and (3) broader distributions. Reprinted with permission from Baranov *et al.*, Rev. Mod. Plasma Phys. 3, 7 (**2019**) [88]. © Springer-Nature.

TIHTUS which is a water-cooled version of the 100 kW radiatively cooled thermal arcjet HIPARC-R, where a segmentation was successfully employed [95]. Moreover, there is an important technical aspect related to the propellant flexibility for hot cathodes in a steady-state operation, since segmented electrode packages can enable the insertion of chemically aggressive gases that then can be used as an amended propellant mass flow rate [88]. Importantly, the described systems were used as plasma generators for aerothermodynamic testing but they demonstrated the supply of gases such as CO_2, O_2 and CH_4 downstream using a neutrode. This aspect also enables in-situ resource utilization by the use of waste gases *e.g.* in long-term manned missions in order to produce additional momentum independent from whether the gas ensures the optimal operation or not. Not surprisingly, the influence of the magnetic field on the characteristics of micro-cathode thrusters and similar plasma sources has recently attracted significant attention from researchers [96–101]. Moreover, other attempts to enhance the parameters of micro-cathode thrusters were focused on the alternative configurations of the discharge system, along with the configuration of magnetic field. Tian *et al.* recently studied several systems with segmented anodes, see Fig. 3. In this research aimed to enhance the characteristics of μCAT thrusters, the structure of electrodes was studied. One of the thruster designs incorporated a cathode shaped as a truncated cone, a sleeve made of insulating material, and a complex anode that was a set of segmented insulated parts (segmented insulated anodes, or SISA-μCAT) including both distant and proximal anodes. The authors of this study established the effects of structure on the discharge parameters, breakdown characteristics, as well as performance for the SISA-μCAT, SEA-μCAT (a segmented exposed anode), and NSEA-μCAT (incorporates a non-segmented exposed anode). The comparison revealed the better performance of plasma ejection system for the SISA-μCAT, that is conditioned by the specially designed electric field generated between the segmented anode and parts on the anodic insulation. For a single ignition of the SISA-μCAT, the maximum thrust was increased by 11.4 times, the maximum thrust-to-power ratio increased by 10.4 times, whereas the maximums of propagation speed and plasma density were increased by 2.93 times and 8.2 times, respectively, when compared to the NSEAμCAT [99]. Such a significant enhancement of the most important thruster characteristic, namely a thrust and thrust-to-power ratio, of particular importance for small satellites, makes this technology very promising and a promising candidate for further development [17].

3.3. Segmented (staged) thrusters

Zolotukhin *et al.* performed a comparative study on the characteristics of *two-stage (segmented) microcathode arc MPD thrusters* with different magnet systems, namely (i) based on permanent magnets, and (ii) powered pulsed magnetic field (Fig. 4) [95]. The permanent magnet-based system is simpler and does not require power but has apparently limited controllability and flexibility. On the other hand, the thruster fitted with the magnetic coil powered from a separate PPU (yet from a single signal generator to synchronize all processes in the discharge) provides many more options for the independent adjustment of the external magnetic field. Importantly, these micro-cathode thrusters are two-staged, *i.e.*, feature additional accelerating electrodes powered by separate PPUs capable of generating voltage pulses of about 60 V, triggered by the same signal generator. Figs. 4a and b show schematics of the thrusters without power and signal circuitry for simplicity [103].

The authors observed that the thrust can exhibit a ten-fold increase for both magnetic field configurations when the second stage is powered at a specific voltage. The pulsed current improves control of the magnetic field, yet produces a delay between the plasma ignition in both stages, and in doing so restrains the possible thrust increase [94]. Permanent magnets allow for the obtainment of a stable increase in the thrust yet at the cost of flexibility of the magnetic field control, a significant drawback for application in micro-satellites [104]. At the same time, the level of electromagnetic emission with a moderate amplitude occurs in a low-frequency range of tens of kHz. The mechanical noise is 100 times lower than the thrust in the normal operating mode for both configurations of the magnetic field. Moreover, the change in the voltage applied to the accelerating electrode does not significantly affect the thrust-to-power ratio, efficiency, or thrust, when the magnetic field is not applied. In summary, these findings show the improvements in the performance of low-power MPD thrusters by the generation of the magnetized arcs promoted by the increase above a specified threshold

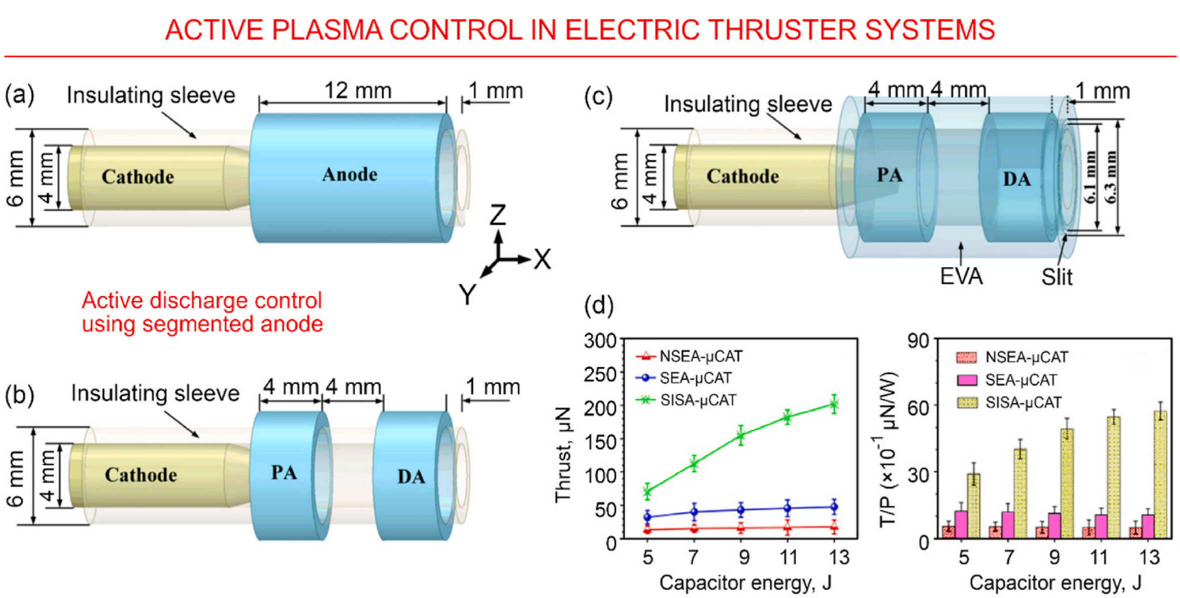

Fig. 3. Active discharge control using segmented anode. (a–c) Structure diagrams and parameters of the three μCATs using NSEA, SEA, and SISA configurations, respectively. (d) Thrust and thrust-to-power ratios produced by the three different μCATs in a single shot. The system with a segmented anode (SISA-μCAT) demonstrates a significant enhancement in thrust and thrust-to-power ratio due to the special spatial electric field between the segmented anode and the slit structure. Reprinted with permission from Tian *et al.*, Plasma Sources Sci. Technol. 29 (2020) [102]. Copyright IOP.

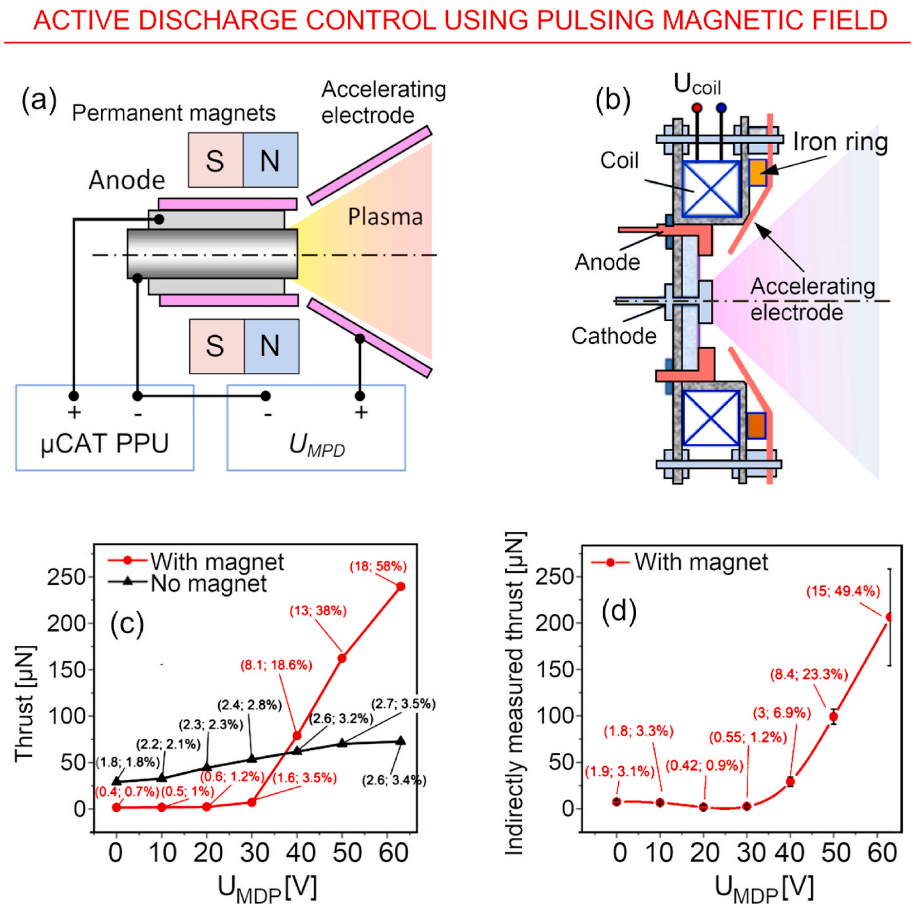

Fig. 4. Active discharge control using pulsing magnetic field and accelerating electrodes. Schematics of the µCAT-MPD thruster with a permanent magnetic ring (a) and a pulsing magnetic coil (b). Reprinted with permission from Zolotukhin *et al.*, J. Phys. D: Appl. Phys. 54 015201 (**2021**) [95]. Thrust, estimated from the electrical measurements of the thruster in with magnet and no magnet configurations (c), and an indirectly measured thrust using the thrust stand in a configuration with magnet (d). The first numbers in brackets is the mean thrust-to-power ratio (in µN/W), and the second ones with percent signs mean efficiency, for the respective data points. Reprinted with permission from Zolotukhin *et al.*, Phys. Rev. E 102, 021203(R) (**2020**) [94].

level of the voltage applied to the second MPD thruster stage.

3.4. Active discharge control using a segmented magnetic coil

Fig. 5a illustrates the scheme for an *active discharge control using a segmented magnetic coil*. The thruster is fitted with an additional (focusing) magnetic coil which significantly influences the discharge. Figs. 5b and c shows the results of the numerical simulation of the discharge for different currents in the focusing magnetic coil. Fig. 5d shows the optical photograph of the plasma jet in the experimental setup with a µCAT-like discharge and a focusing magnetic coil. Both the ‘magnetic bottle’ configuration generated by coils 1 and 2, with the same direction of the current, and the ‘magnetic cusp’ configuration obtained by use of the oppositely-powered coils, allows the generation of a region with dense plasma (marked red) [88,105]. Thus, the application of segmented electrodes, segmented multi-stage magnetic coils and their combinations ensure, provided that the due synchronization was achieved, significant intensification of the discharge and essential

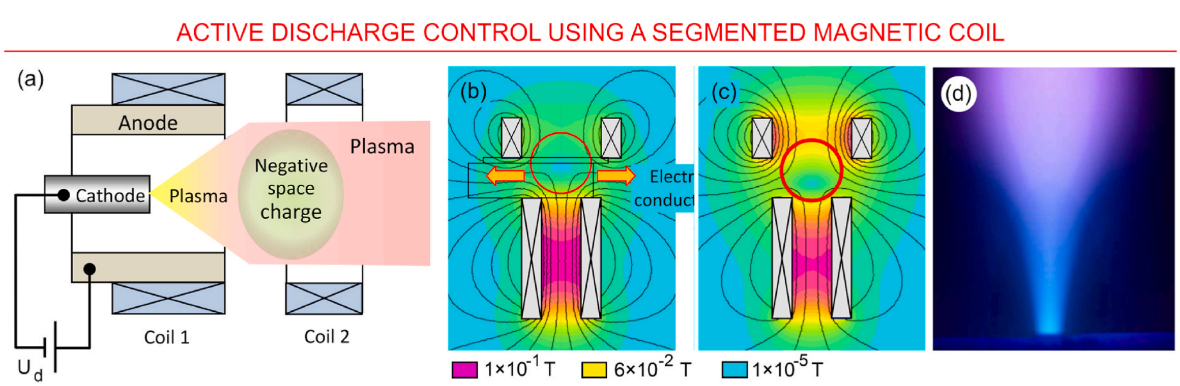

Fig. 5. Active discharge control using a segmented magnetic coil. (a) µCAT with additional (focusing) magnetic coil, and (b,c) numerical simulation of the discharge for different currents in the focusing magnetic coil; (d) optical photograph of the plasma jet in the experimental setup with µCAT-like discharge and focusing magnetic coil. Reprinted with permission from Baranov *et al.*, IEEE Trans. Plasma Sci. 42, 304 (**2018**).

enhancement of the most important characteristics of μ-thrust vacuum arc thrusters. This field is also particularly covered by the developments for electrodeless thrusters where the magnetic field configurations that employ magnetic nozzles are divided into segmented designs, to additionally manipulate the discharge. Correspondingly, in some of these designs even ECR modes are triggered by the magnets aside the general manipulation of the discharge [86,87,89,106]. Among the other institutions actively exploring this field are the University of Madrid, Spain; Institut de Combustion Aérothermique Réactivité Environnement (ICARE), Orléans, France; and Institut für Raumfahrtsysteme (Institute of Space Systems, IRS).

3.5. Active plasma control in vacuum arc thrusters

Active plasma control is important for many types of thrusters *e.g.* the vacuum arc thrusters (VAT) and also for magnetic nozzles [90,91]. VAT is a very low-thrust device that requires many hours of operational time to impart its total impulse. Since a VAT utilizes the cathode electrode as a solid propellant, the cathode is consumed by erosion and requires replenishment. In the pulsed mode of operation, the electrode erosion and very low thrust complicate obtaining statistically meaningful performance results. Recently, a coaxial VAT with an active feeding mechanism was introduced known as the inline-screw-feeding VAT (ISF-VAT) [107,108]. An ISF-VAT prototype was developed at the Technion Institute of Technology to enable large scale data collection and evaluate the performance of VATs. The ISF-VAT was recently used to study the effect of weak magnetic nozzles on VAT performance.

For magnetic fields up to 0.2 T, performance increases over the non-magnetic case are observed with the best thrust-to-arc power ratio ≈9 μN/W obtained at a magnetic field of approximately 0.2 T. A parametric model captures the performance enhancement based on beam collimation and plasma acceleration in the magnetic nozzle [109]. For magnetic fields greater than 0.2 T, the arc discharge is shown to be suppressed, nullifying any additional gains by the nozzle effect.

- ✓ *An* enhancement in *the plasma control in the EP thrusters, the introduction of new control mechanisms and principles would contribute to* a *further* increase in *the operational characteristics, durability and service life of space propulsion systems* [110–113].

4. Recent advances in rotating magnetic field systems

Rotational systems for space propulsion have not been demonstrated in the form of a flight-ready device, but they offer promising features, and thus attract the attention of researchers and engineers working in the area of miniaturized EP thrusters [114,115]. Such systems feature the following main advantages: (i) higher thrust densities conditioned by the absence of limitations intrinsic to gridded ion- or Hall-type thrusters, dependence of the acceleration process on electrical screening or Hall parameter; (ii) absence of a neutralizer, (iii) thruster throttling between the higher thrust and specific impulse, while maintaining the constant power, and (iv) removal of electrode material erode that is accompanied with plasma contamination and lifetime limitation, *e.g.,* referring to cathodes.

4.1. Rotamak-type systems

Recently, several novel techniques have been demonstrated that bring the rotational systems close to space implementation. As an example, a spherical plasma source Rotamak (GER) initially developed for the controlled thermonuclear fusion in The Space Propulsion Centre (SPC) in Singapore at the Nanyang Technological University, has successfully passed the preliminary tests to be applied as a prospective device for plasma propulsion, *i.e.* as a small space thruster [116]. The experimental results of the study on the Rotamak-type (GER) device were reported. This system is characterized by a configuration where an azimuthal plasma current in a compact torus is guided by an external rotating magnetic field (RMF), and an external steady axial field keeps the current at an equilibrium. When the azimuthal current exceeds a specified value, the steady field is reversed to generate a field-reversed configuration (FRC). Figs. 6a and b show the 3D model of the Rotamak coils, as well as the configuration of the magnetic field of the device, where the toroidal magnetic field is depicted with dashed curves. Fig. 6c is the optical photograph of the operating GER system. When deployed in space as a miniaturized thrust system, the electrodeless Rotamak-like thrusters (see Figs. 6d and e for the suggested design) could be a possible solution for the problem of electrode erosion that Hall and gridded ion thrusters suffer.

Fig. 6f shows quite high plasma density, greater than 10^{19} m^{-3}, that has been demonstrated in the experiments with the azimuthal current reaching 4 kA at 400 W of total RMF power, thus proving the possibility of designing a “pure electromagnetic” thruster to generate high-density non-inductive plasmas. This type of thruster is assumed to generate the azimuthal plasma currents to cause non-selective acceleration of ions, electrons and neutrals by use of an axial body force. Thus, the necessity of implementation of additional elements of design such as the stages for preliminary ionization, grids or neutralizers is omitted, unlike for the commonly used types of thrusters. Moreover, the flexibility of operational power control, significantly decreased erosion of structure elements, as well as the absence of moving parts of the structure benefit further development of the device suitable for application as in deep space missions as in lower Earth or geostationary orbit missions. Thus, the ability of the miniaturized Rotamak system was proved. It was demonstrated that the characteristic processes occurring in the rotating magnetic field device with respect to the generation and acceleration of particles, allows considering Rotamak as a novel platform for space exploration. Further efforts should be put with a purpose of development of a sample for the flight operation tests.

4.2. Helicon antenna-based plasma source

Fig. 7a shows a similar scheme but with a helicon antenna-based plasma source and the divergent magnetic field in the RMF acceleration area [117]. The axial ion velocity of 3 km/s was achieved, the rate of density increase was 70% for the RMF frequency of 3 MHz. To confine the electrons and make them rotate azimuthally by the RMF, the RMF frequency was set in a range between the cyclotron frequencies of ions and electrons. This resulted in the generation of the azimuthal electron current. Argon propellant was supplied through a flange of quartz tube to be ionized in a helical device enhanced by a set of permanent magnets with a specially designed cover of stainless steel for an external diverted magnetic field. The configuration and strength of the magnetic field conditioned the axial position of RMF antennas; the application of the divergent configuration of the magnetic field necessary for the plasma acceleration is considered. The RF antenna was powered with pulses of a duration of 75 ms separated with a 1.5 s time lap, and the RMF was applied in 35 ms after plasma ignition. The effect of a rotating magnetic field is clearly seen in Fig. 7b where the measured distribution of electron density in plasma and ion velocity are shown. Significantly higher electron density and ion velocities were reached with the application of RMF with a frequency of 0.7 MHz, when the electron density reached its central peak upstream of the RMF antennas. These highly promising results inspire further research efforts in this field [118–121].

Apart from the thrusters that exploit the rotational modes, similar effects have been recently discovered in cathodes that are used in Hall-type and gridded ion thrusters. Becatti *et al.* have recently reported the observation of the rotating magnetohydrodynamic modes in the plumes of high-current hollow cathodes [122,123]. Rotational instabilities and regimes were previously reported for various types of thrusters, including Hall type systems [124,125]. The discovery of rotational modes in the cathodes will enable the finer optimization of this critically important sub-system of EP thrusters. Fig. 8 shows the scheme of the

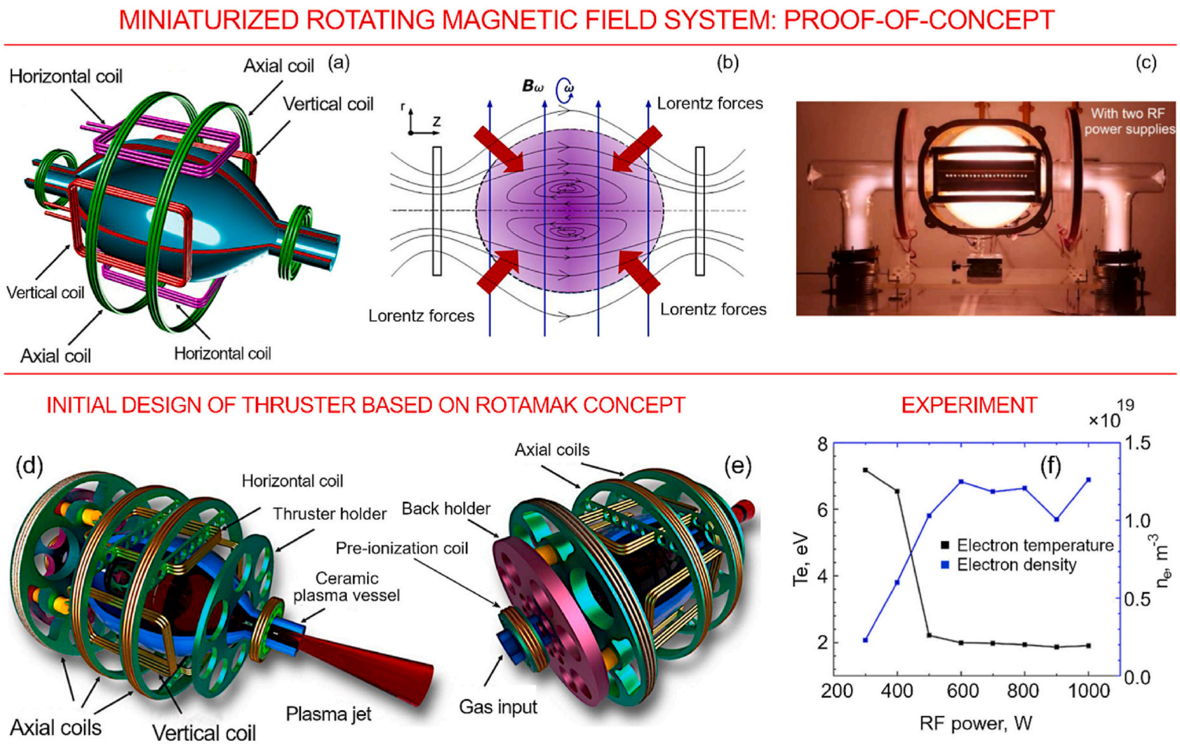

Fig. 6. Systems with rotational effects. (a) 3D schematics of the main coils in the Rotamak system. (b) Magnetic field configuration of a compact torus device. (c) Optical photograph of operating GER system. (d,e) Initial design scheme of the practical thruster based on the Rotamak concept (under development). The design consists of three axial coils and two holders joined with cross-plates to form the main frame, where the plasma vessel is installed. Additional coils, together with gas supply pipes and insulating inserts, are fixed within the frame. (f) Experimental dependence of electron temperature and electron density on the radio frequency power in GER system. Reprinted with permission from Sun *et al.*, J. Phys. D: Appl. Phys. 30, 065003 (**2021**).

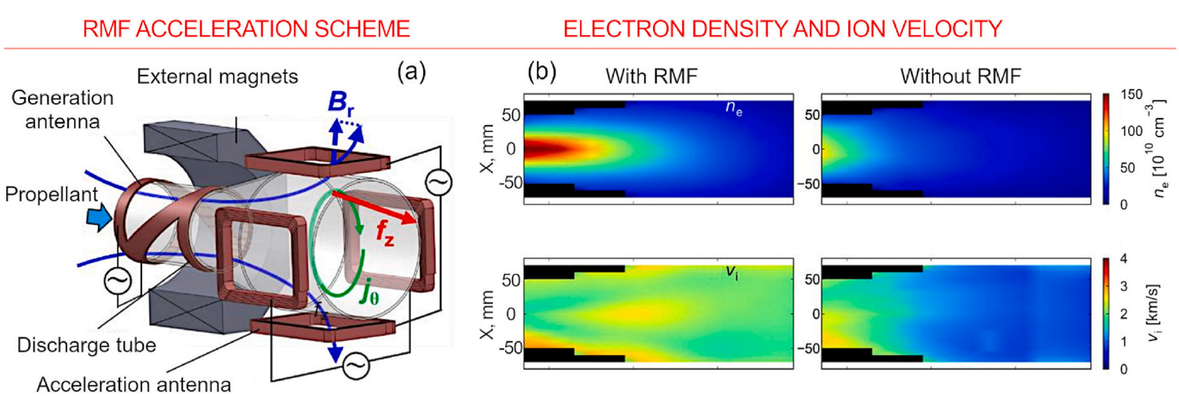

Fig. 7. (a) Schematic view of the rotating magnetic field coils in the system with the divergent magnetic field. (b) Measured spatial profiles of electron density and ion velocity in the RMP device with a divergent magnetic field. Reprinted with permission from Furukawa *et al.*, AIAA 2020–3630 (**2020**) [114].

cathode and three frames from the high-speed video.

4.3. Rotational modes in cathodes

Hollow cathodes that are capable to generate high currents are widely employed for space propulsion. However, a large set of fluctuations could be observed in the region that is located in the close proximity to the cathodes, thus leading to generation of the coherent plasma structures that greatly affect the performance of the cathode [120,126]. When a hollow cathode operates in a continuous mode, the plasma instabilities are developed in the exterior of the plasma plume region and also deteriorate the performance of the whole thruster unit, and even could result in its complete shut-down. Moreover, the instabilities in plume generate energetic ions that are responsible for the intensive erosion of structure elements in the near cathode region, thus causing the damage of the structure. Becatti *et al.* revealed the existence of MHD azimuthal mode with a frequency of 58 kHz, by use of Fast-Cam images (Fig. 8b) collected in the exterior region of the hollow cathode that operated at 25–150 A in the presence of an axial magnetic field. The ideal magnetohydrodynamic theory that takes into account the boundary condition of a non-line-tying cylindrical anode, predicts the mode, its measured frequency and the wavenumber. These results contribute to the deeper understanding of the physics of a hollow cathode systems and thus will facilitate designing of the high current, long operating cathodes for powerful electric propulsion thrusters need for the future interplanetary missions.

Of interest for future thrusters is harnessing the energetic ion generation observed in these high-current plasma discharges. Ion

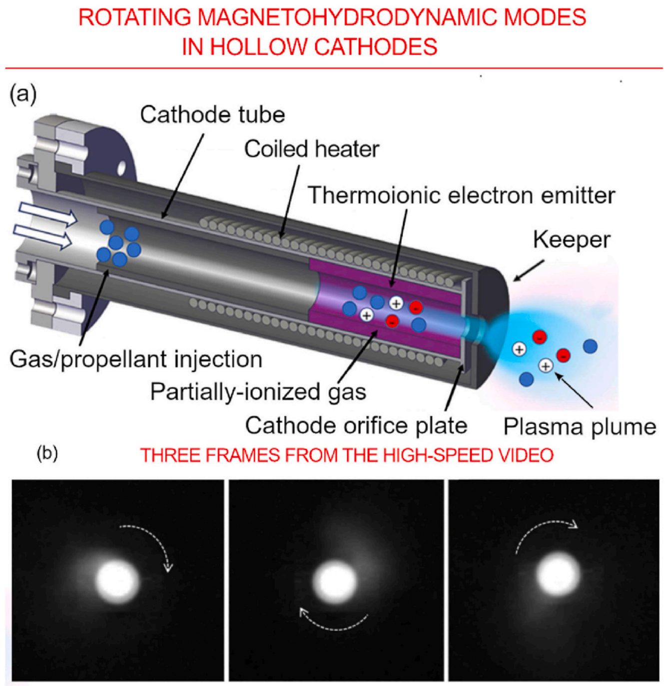

Fig. 8. Rotating magnetohydrodynamic modes in hollow cathodes. (a) Hollow cathode schematic showing the basic components and plasma location. Reprinted with permission from Goebel *et al.*, J. Appl. Phys. 130, 050902 (**2021**). (b) Sequence of three frames from the high-speed video from the cathode front. Reprinted with permission from Becatti *et al.*, J. Appl. Phys. 129, 033304 (**2021**) [119].

acceleration by MHD waves has been described by Miller [127] and Petrosian & Liu [128]. In addition, Drake *et al.* described ion heating and acceleration during magnetic reconnection [129]. They showed that ions above a critical mass-to-charge ratio behave like pickup particles (particles in a local plasma flowing at the Alfven speed) as they enter the exhaust region of a flare and thereby gain significant energy. The exploitation of similar physics that uses rotational waves or magnetic reconnection for the acceleration of ions from these hollow cathode discharges could enable a new class of electric thrusters.

5. Innovations in alternative propellants and propellant supply systems

Propellants are a very important part of the space thrust systems, and the requirements for the specific propellants are quite dependent on the type of a thruster and the physical principles it is based on. While some types require heavy gases with acceptable physical properties in the terms of plasma formation (*e.g.,* ion thrusters including Hall-type platforms), other e.g. thermal arcjets require light propellant for the best performance. Since ion thrusters are currently very popular and massively used on satellites (*e.g.*, Hall-type thrusters power Starlink satellites), the attempts to find an alternative for very expensive xenon used as a propellant, with a general purpose to improve the cost efficiency of the space exploration projects, were made during the last decades. The systems operating with molecular propellants, iodine, and even water have been recently demonstrated [130–132]. However, xenon is the regular gas applied as a propellant in many Hall thrusters because it possesses an optimal set of chemical and mass properties for the purpose. However, Starlink satellites utilize krypton and the tendency for the replacement of Xe on Hall thrusters continues [57,63,68]. Currently, other materials that are not in a gaseous state at ambient temperature, are considered as propellants for various types of thrusters, and many of them are referred to as "condensable" propellants because of their condensed state opposite to the gaseous propellants.

5.1. Condensable propellant thrusters

Iodine. Recently, D. Rafalskyi *et al.* demonstrated a successful application of an ion thruster utilizing iodine in space, thus offering a cost-effective and simple alternative to xenon and krypton [133]. Fig. 9a shows a simplified scheme of an iodine-based EP system [134]. In this thruster, solid iodine is stored in a tank and heated there forming a gas via sublimation. Next, the gas is fed into the thruster through a tube. Plasma is generated via electron collisions in the radio-frequency discharge, collides with a gas molecule, and produces two electrons and an iodine ion. The following processes are typical for the gridded ion thrusters: the ions are then extracted from plasma and accelerated, and then the ion beam is neutralized by the cathode. When the heating is turned off, a plug is formed by the cooled iodine that is solidified in the orifice that connects the tube to the tank.

The ability of iodine to sublimate from the solid phase when heated makes it possible to place it directly into the thruster, thus avoiding the complex system with high-pressure tanks and feeders. Fig. 9b illustrates

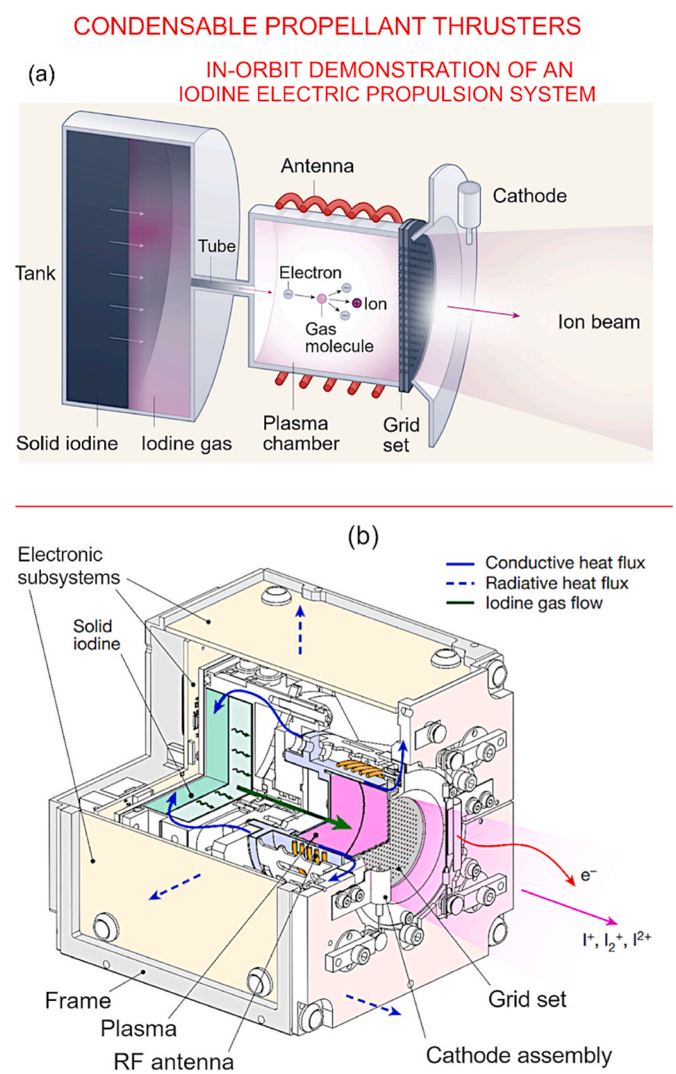

Fig. 9. Innovations in propellants. (a) Simplified scheme of iodine-based EP system. Reprinted with permission from Levchenko et al., Nature (**2021**) [131]. (b) Schematic of the NPT30-I2 iodine EP system. Solid iodine is located in a storage tank upstream of the plasma source tube. Heating causes sublimation. A RF antenna creates a plasma, and a set of grids accelerates iodine ions. Reprinted with permission from Rafalskyi *et al.*, Nature (**2021**) [130].

the schematic of the NPT30-I2 iodine EP system. After the sublimation of iodine, plasma is generated by the use of an RF inductive antenna, and importantly, the *efficiency of the ionization is higher*, as compared with xenon. Then, an accelerated highly-collimated flow of atomic and molecular iodine ions is created by high-voltage grids, and substantial iodine dissociation is observed in the process of thrust generation. The successful implementation of the propulsion system was performed onboard a small satellite, that was confirmed through the data of the satellite tracking. These results can be considered as a powerful argument for the early application in the space industry the alternative propellants similar to iodine. *Iodine could enable significant simplification and miniaturization* of the propulsion systems, thus increasing the performance of the thrusters with respect to all aspects of their application [135,136].

However, there are some limitations in the application of iodine as the propellant, that are caused by its corrosive nature that creates a potential danger for the satellite systems. That is why complex ceramics and polymers were engaged in the developed system to protect the structural elements made of metals. Moreover, a matrix made of a porous aluminum oxide was used to carry the iodine crystals, which increased the mass and complexity of the system. Although these drawbacks should be addressed before the implementation of the whole concept into the satellite industry, the system with iodine can be considered a breakthrough in EP.

Thrusters operating on naphthalene and elemental bismuth. Fig. 10 and 11 explore recent efforts on designing and testing an experimental setup with a thruster operating using naphthalene as a propellant [137]. Naphthalene is a promising propellant due to its operational characteriastics and properties. Similar to iodine, the temperature for naphthalene sublimation is relatively low, producing a vapor pressure that is sufficient to support a useful mass flow rate for a small thruster. Elemental bismuth has also been used as a propellant for Hall thrusters [138]. A hollow anode with heating was engaged to produce the vapor at the chamber inlet and distribute it around the thruster axis; the results were compared with the data obtained for xenon used as the propellant. It was confirmed that *bismuth allows obtaining a significant increase in the ratio of thrust to discharge power* for the discharge voltage drops of 250–400 V; the same trend was observed for the anode efficiency.

In the experiments, the shape of the plume was almost the same for both gases [138]. The measurements also confirmed that the difference between the theoretical speed and mean velocity is much less for bismuth, which implies that propellant utilization is lower for xenon, while it provides a bit higher specific impulse. Furthermore, the shapes of the central plume are almost the same, as was proved by the measurements of current in the ion plume. In addition, the experiment revealed the difference in the charge exchange mechanism for ions at large angles, where the population was much higher with xenon. Thus, it can be stated that the shape of the plume for bismuth is not affected significantly by the changes in thruster operation modes. In general, elemental bismuth is a very promising replacement for xenon, ensuring a significant boost in many thruster characteristics and a much lower price. However, the energy required for bismuth evaporation along with the complexity of the bismuth supply system are the factor that currently hinder the wide application of bismuth and iodine.

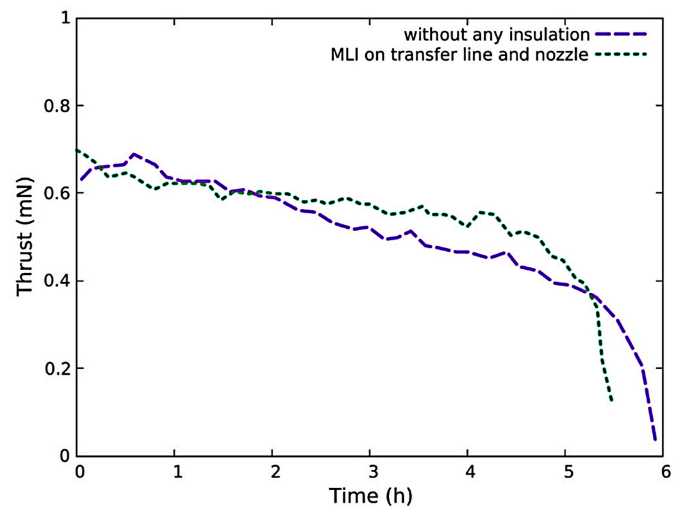

Fig. 11. Thrust measured over time. The thruster was set to perform 12 s burns in minute, with the reservoir maintained at a temperature of 70°C. Initially, the reservoir contained 10 g of naphthalene and the system operated continuously until the propellant was depleted. The purple dashed line represents data taken without insulation on the transfer line and nozzle, while the green dotted line shows results after the transfer line and nozzle were insulated with multi-layer insulation (MLI). Reprinted with permission from Tsifakis et al., Front. Phys. 8, 389, 2020 [137] under the terms of the Creative Commons Attribution License (CC BY).

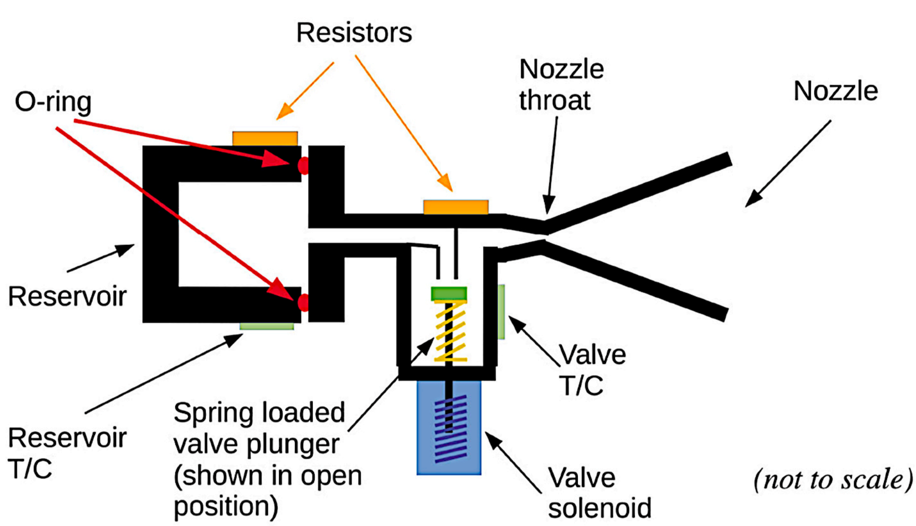

Fig. 10. Schematic of the naphthalene thruster, illustrating its key components. The reservoir temperature (Tr) is monitored by the reservoir thermocouple (T/C) and maintained by the reservoir heater resistor. Similarly, the valve temperature (Tv) is tracked by the valve thermocouple (T/C) and regulated through the valve heater resistor. Reprinted with permission from Tsifakis et al., Front. Phys. 8, 389, 2020 [137] under the terms of the Creative Commons Attribution License (CC BY).

Metals as propellants. Figs. 12a and b illustrate the metal plasma thruster (MPT) for driving micro- and nanosatellites. This type of thruster utilizes propellants made of solid metals, moving parts are not engaged in the design. The device generates approximately 5000 N × s/U, and typical packages are ½-U, 1U, and multiple-U increments. The vacuum arc accelerates the plasma plume up to velocities of 6.8 km/s (platinum, Pt) or even 30.6 km/s (magnesium, Mg) followed by generation of thrust of about 10 μN/W. Thus, the thruster is powered from a DC source of 7–28 V and controlled by pulses supplied from the satellite bus; therefore, the total impulse per mass unit of the propellant is high.

The design is simpler than Hall and ion thrusters and allows scaling it down. After comparison with other types of thrusters of the same size range, such as xenon gas RF thruster, field emission EP thruster, and pulsed plasma thruster, the authors made a conclusion about more flexible operation of MPTs. Fig. 12c shows the shape of arc discharge pulse of the MPT thruster. However, the operation using zinc propellant still has not been demonstrated, yet the zinc vapor feeding system is currently under development [141].

Metallic propellants are also used in the prospective laser-electric hybrid space thruster systems which are currently under development [142,143]. The method of laser-enabled space propulsion features several significant advantages such as very high thrust-to-power ration and high specific impulse [144,145]. Schematics of the laser-electric hybrid thruster are illustrated in Fig. 12d. In this system, the ablation in the focus of a laser beam is used to vaporize or decompose the propellant. The plasma then can be accelerated by electromagnetic forces to produce the thrust. This kind of thrusters features many additional advantages due to the separate plasma generation and accelerated processes. In a thruster of this type, the parameters of laser-assisted ablation along with the parameters of plasma acceleration influence the thrust and characteristics of the thruster. This type of dual control ensures higher accuracy in controlling the thrust pulses, thus ensuring precise maneuvering and attitude adjustment for the satellites. Not surprisingly, extensive works on these thrusters are in progress. In particular, the behavior of various metals is being studied, including copper, steel and aluminum, in the prospective laser-electric hybrid space thruster [138]. The dependencies of ablated mass on the type of metal for various pulse energies are shown n Fig. 12e. The comparison has demonstrated that the copper ensures the most uniform distribution of plume. On the other hand, aluminum ensures faster expansion of plume ablated by nanosecond laser, thus faster response of the thruster utilizing aluminum. As expected, higher laser energy results in the higher ablated mass for all metals. However, some saturation of the ablation rate could be noticed, possibly due to the shielding of laser beam with plasma. Fig. 12f shows the dependence of plume velocity, *i.e.*, the specific impulse, on laser pulse energy for three types of metal propellants. The plume velocity for Al was the highest, as compared with the steel and copper.

Since the absence of gas storage and supply systems, along with advanced discharge characteristics intrinsic to the condensable propellants are strong advantages for the miniaturized space propulsion systems, many teams and companies are currently exploring this type of propellants [146–148]. Examples are the Ion Space Propulsion Laboratory at Michigan Tech where Hall thrusters with condensable propellants are being developed since 2004. A specialized facility to test the thrusters fueled with zinc, bismuth and magnesium was used to investigate the operational characteristics of the thrusters. All the metal propellants exhibited superior performance accompanied by significant cost reduction compared to the commonly used xenon propellant. The unique process of the vaporization of the propellants by use of waste heat supplied from the plasma discharge was patented by Michigan Tech

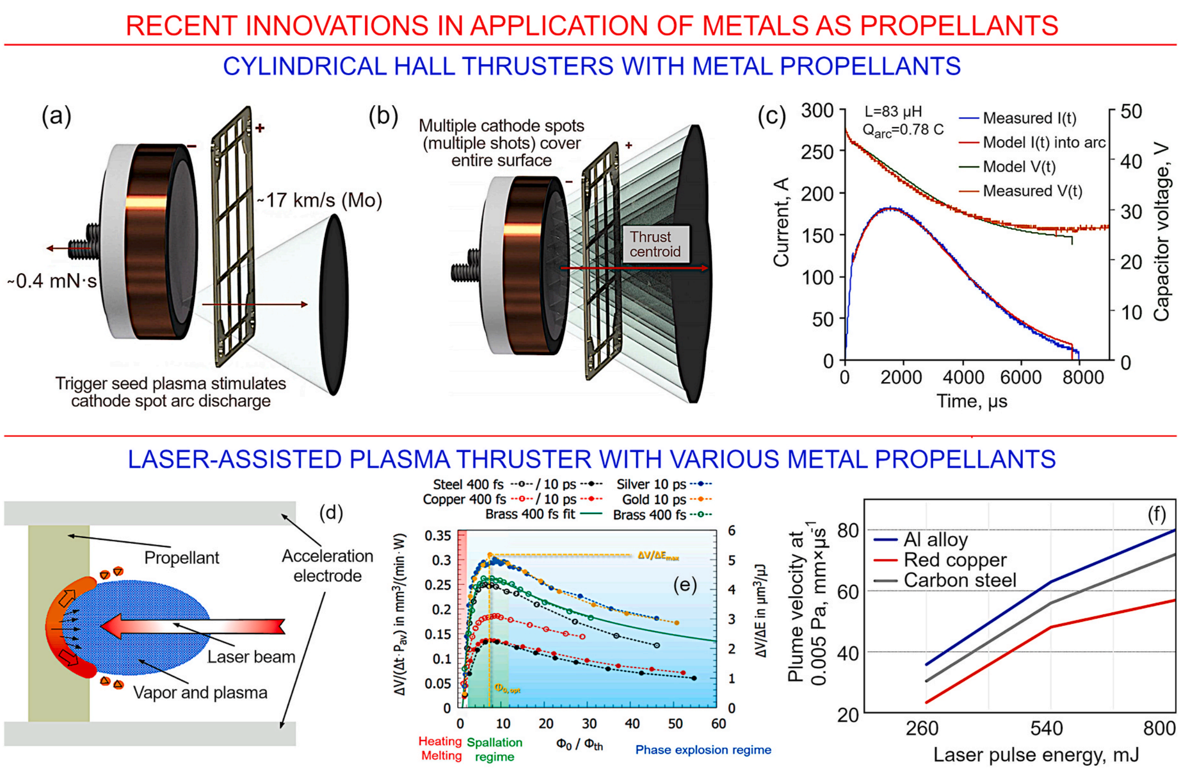

Fig. 12. Recent innovations in the application of metals as propellants for space thrusters. (a,b) Scheme of the metal plasma thruster (MPT), and the shape of arc discharge pulse of the MPT thruster (c). Reprinted with permission from Krishnan *et al.* [135]. Copyright AIAA 2020. (d) Schematics of laser-electric hybrid thruster where metals could be used as propellants. Reprinted with permission from Ou *et al.* [139]. Copyright Elsevier 2022. (e) Dependence of ablated mass on the type of metal for various pulse energies. Reprinted with permission from Yuanzheng *et al.* [140]. Copyright IOP, 2021. (f) Plume velocity (specific impulse) for three types of metal propellants. Data from Ref. [138]. (e) Energy specific volume for a single pulse laser ablation obtained in laser milling experiments. The fluence along the x-axis is normalized to the ablation threshold for respective metals. Reprinted with permission from Forster *et al.* [140] under the terms of a Creative Commons Attribution 4.0 International License.

[149]. Another example is the Plasma Sources and Applications Centre/Space Propulsion Centre Singapore that has recently demonstrated the krypton Hall thruster [57] and is currently developing the iodine propelled miniaturized Hall thruster [150], and the Busek company that presents a line of Hall thrusters ranging from 100 W to 20 kW, capable of operating using iodine, along with xenon and krypton [58,151].

5.2. Thrusters with composite and nanoparticle-doped propellants

Composites doped with metal oxides as propellants. Along with the metallic propellants, complex and composite materials with various dopants and nanoparticles are also currently under extensive investigation as propellants for space thrusters. Figs. 13a and b show the scheme of laser-electric hybrid thruster utilizing polytetrafluoroethylene (PTFE) propellant filled with various dopants, and the optical photographs of the plasma [149]. Since the propellant is ablated with the laser beam, it can be non-conductive in contrast to pulsed thrusters where the material of the electrode is used for acceleration via electromagnetic forces. Importantly, dopants play a very significant influence on the thruster characteristics and in particular, on the specific impulse as illustrated in Figs. 13c–e. While doping with Co–Cr ensures only 800 s, doping with NaCl rises the impulse to 4000 s and doping with TiO_2 ensures 8000 s. Rate of doping also significantly affects the specific impulse, together with the initial voltage.

Metal oxides are promising dopants for the laser-electric hybrid thrusters, which are currently under extensive investigation. Figs. 14a and b show the dependence of plasma plume area for the experimental laser-electric thruster utilizing PTFE propellant dopped with various metal oxides including CuO, NiO, VO_2, and Fe_2O_3 [136]. Fig. 14c shows the scheme of the experimental setup. The type of metal oxide strongly affects the development of the plasma plume, and the percentage of metal oxide in PTFE should be optimized to ensure the best plasma generation conditions (Fig. 14b).

Nanocarbon and graphene as propellant dopants. Nanocarbon, graphite and graphene also could be used as promising propellant dopants for laser-electric thrusters. Fig. 14d shows the optical photograph of the prototype thruster utilizing carbonous propellants, and Figs. 14e and f show the dependencies of specific impulses on laser power for various doping ratios of nanocarbon and graphene. Doping ratios significantly influence the specific impulse, which exceeds 1000 s for graphene. Specifically, the authors demonstrate that the 5% doping ratio on PTFE is optimal for carbon and graphene [151]. This finding was explained in terms of optimal density of doping particles which absorb the laser power and transfer it to the polymeric matrix, thus ensuring ablation of the polymer. Dependencies of the specific impulse on laser power for various types of dopants demonstrate that the impulse for carbon dopant features some saturation with the laser power while the impulse for graphene strongly rises with the power.

5.3. Innovations in propellant supply systems

Internal Gas Feeding. Recently, Shinohara *et al.* have demonstrated a strong influence of the propellant gas supply method on the discharge characteristics of electrodeless plasma thrusters. Figs. 15a and b illustrate the technique of (a) Conventional Gas Feeding (CGF) and (b) Internal Gas Feeding (IGF) [154]. In the IGF method, the gas is supplied to the thruster close to the discharge zone, via the supply tube placed in the discharge chamber. Figs. 15c and d show the differences in the profiles of electro and neutral particle densities measured for these two methods, and profiles of pressure along the center line of the thruster. As one can see from these graphs, the differences are quite significant, and IGF features strong peaks of the plasma and neutral particle densities at the thruster center line. Importantly, IGF demonstrates a strong electron density peak while CGF shows a flat distribution with a depletion of neutrals near the axis.

Vertex-type propellant supply. Two decades ago, experimental investigations proved that the tangential gas injection is the best method ensuring better parameters of the inductively heated plasmogenerators [155]. Not surprisingly, similar technology is now adapted for various types of plasma-based thrusters, and the recent results are quite promising. In particular, the vertex-type gas propellant supply could be very promising for the miniaturized cylindrical [156] Hall thrusters. The

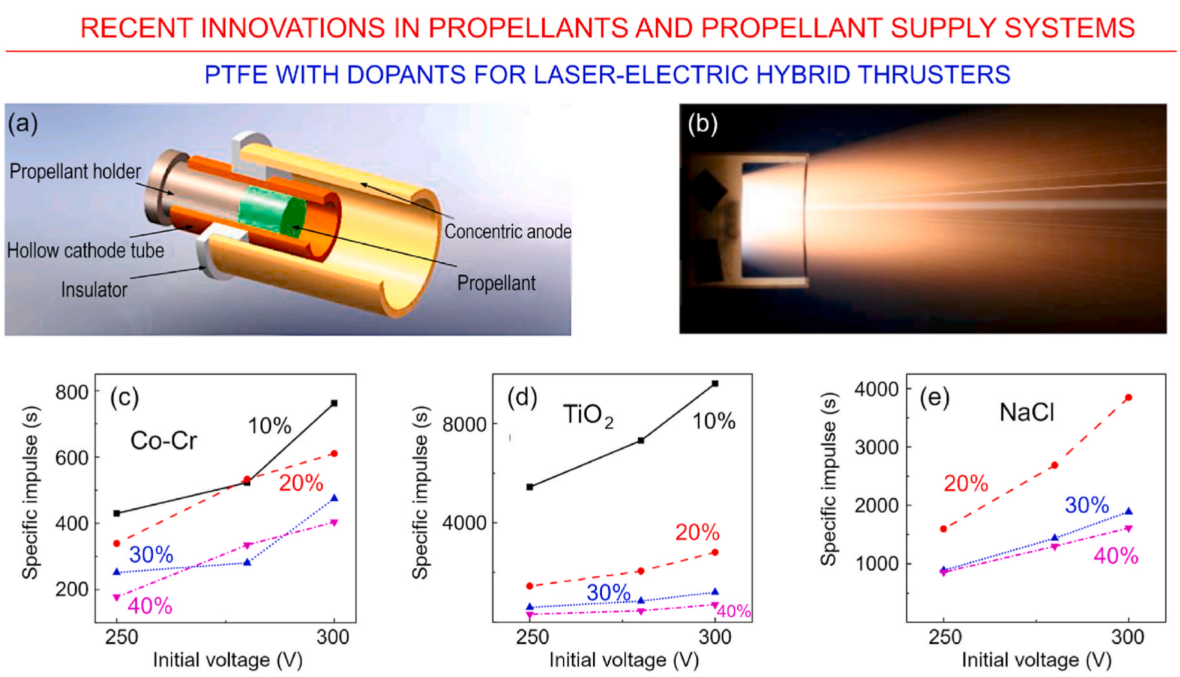

Fig. 13. Application of complex and composite materials as propellants for space thrusters. PTFE with various dopants for the laser-electric thrusters. (a) Schematics of laser-electric hybrid thruster, and (b) optical photograph of the operating thruster. (c–e) Specific impulse as a function of initial voltage for the PTFE doped with Co–Cr (d), TiO_2 (e), and NaCl (f). Reprinted with permission from Ou *et al.* [152]. Copyright Elsevier **2021.**

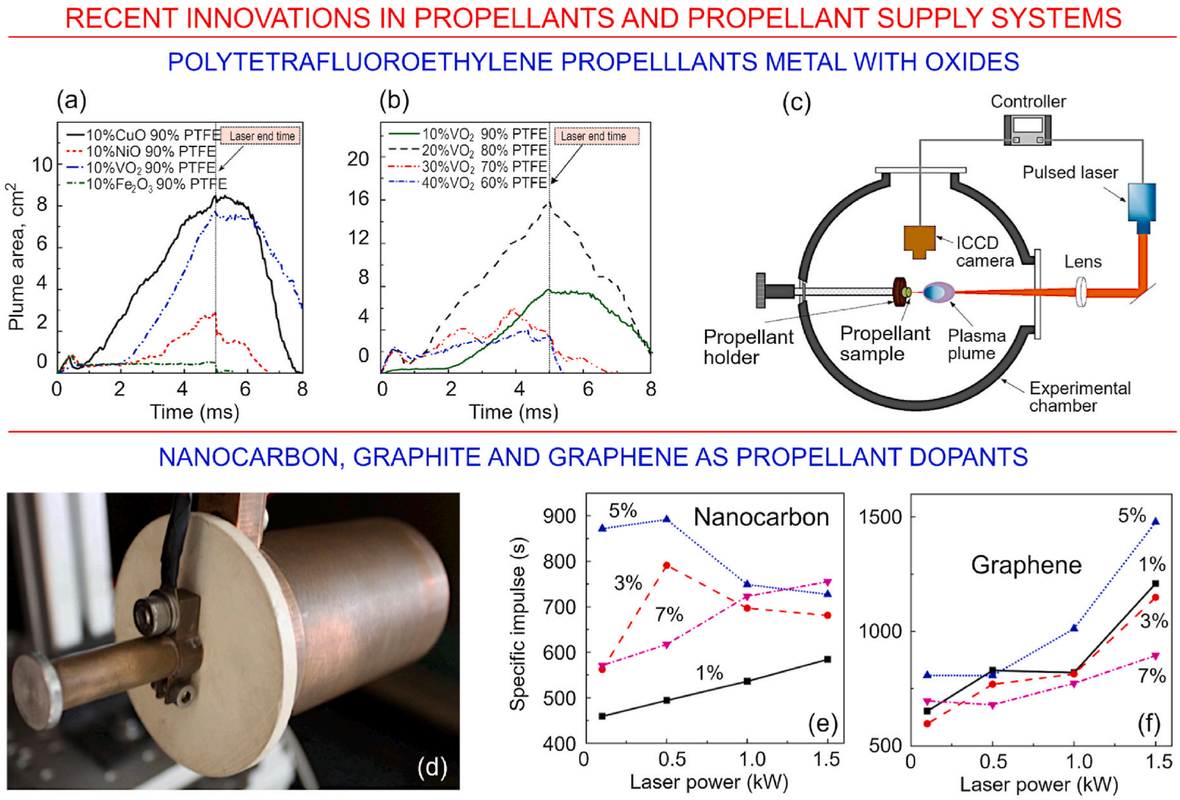

Fig. 14. Application of complex and composite materials as propellants for space thrusters. (a,b) Plasma plume area for the experimental laser-electric thruster utilizing PTFE propellant dopped with various metal oxides including CuO, NiO, VO_2, and Fe_2O_3. (c) Schematics of the typical experimental setup for the characterization of laser-electric thrusters. Reprinted with permission from Ou *et al.* [136]. Copyright Elsevier **2022**. (d–f) Application of carbon, graphite and graphene as propellant dopants for laser-electric thrusters. (d) Optical photograph of the prototype thruster; (e,f) specific impulses as functions of laser power for various dopant ratios of carbon (e) and graphene (f). Reprinted with permission from Ou *et al.* [153]. Copyright Elsevier **2022**.

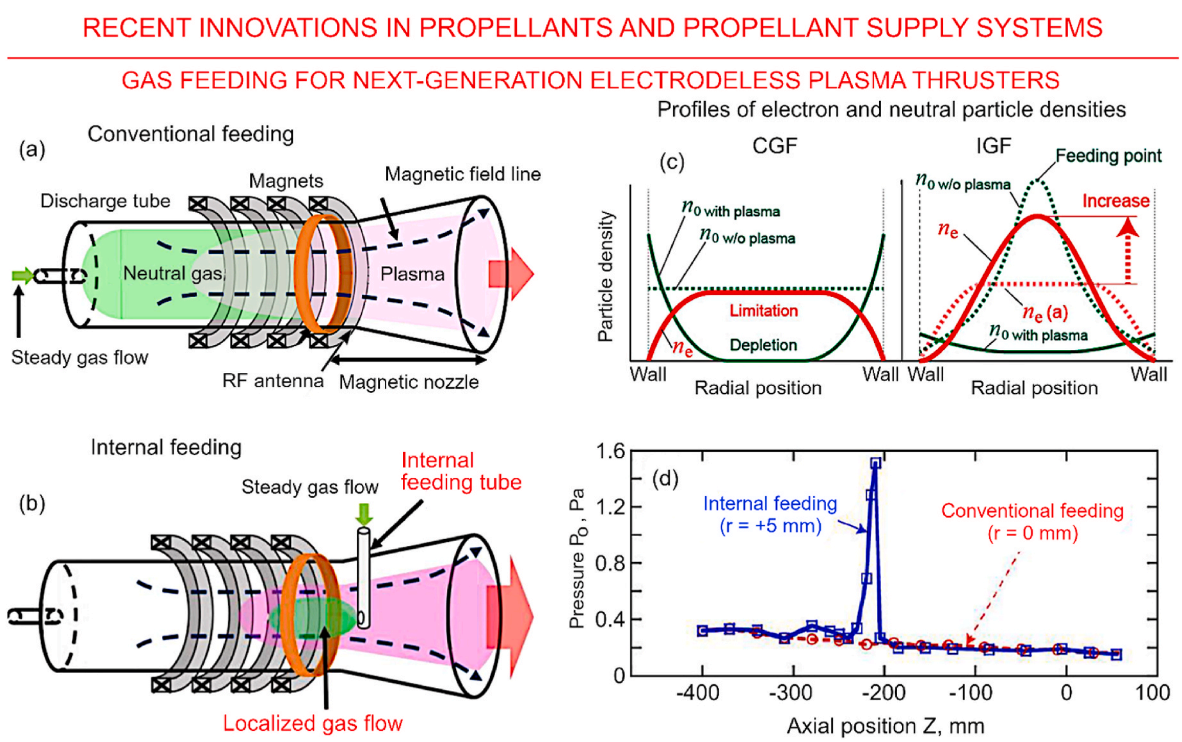

Fig. 15. Innovations in propellant supply systems. Methods of (a) Conventional Gas Feeding (CGF) and (b) Internal Gas Feeding (IGF). (c) The radial profile of electron and neutral particle densities for CGF and IGF modes. A significant increase in density is noticeable for IGF mode. (d) Pressure profile near the center axis for CGF and IGF modes. Reprinted with permission from Shinohara *et al.*, Rev. Sci. Instrum. 91, 073507 (**2020**).

study by Ding *et al.* [157] presents a new design of the propellant inlet for a cylindrical Hall thruster operating at low power, which supports the mode designated as "vortex inlet". The gaseous propellant is supplied as a circumferential vortex to the discharge channel, which allows for increasing the density of the neutrals and extends the dwell time for the gas in the channel, as was confirmed by the experiments and simulation. Fig. 16a compares the designs of conventionally used radial supply with the vortex-type supply system. As seen from Fig. 16b, the distribution of neutrals density at the inlet is much less uniform in the conventional radial supply mode, where the gas is concentrated in the center of the discharge channel, and then expands in the axial direction. In addition, the density of the gas propellant is higher near the anode where it is injected. The motion of the gas in the vortex is changed directly around the surface of the anode. The circumferential motion in the vortex is formed by a tangential gas flow rate; a peripheral diffusion is stimulated by a centrifugal force. The measurements show that the vortex design improves the performance characteristics: 3.12%–8.81% are added to the propellant utilization, 1.1%–53.5% – to thrust, 1.1%–53.5%, – to specific impulse, 10%–63% – to thrust-to-power ratio, and 1.6%–7.3% – to anode efficiency.

Fig. 17a presents the characteristics of the optimized krypton Hall thruster with vertex-type and conventional radial propellant supplies [158]. The relatively low ionization performance of krypton is conditioned by its small cross section for ionization, thus resulting in lower specific impulse, when operating in Hall thrusters instead of xenon. The author also used a rotating mode to supply the propellant through the gas distributor, which changes the distribution of neutrals in the discharge. To study the effect, the dependencies of the discharge current on the discharge voltage, magnetic field, and flow rate were experimentally measured.

It was shown that the application of the rotating propellant reduces the effective axial velocity of the neutrals and increases the circumferential motion distance and density; in total the ionization efficiency of Hall thrusters operated on krypton increases due to this mode. Moreover, the thrust and efficiency also increased, and the divergence angle of the plume is reduced after the implementation of the design modification. Under some conditions (discharge voltage and flow rate), the anode efficiency is increased from 46.2% to 53.2%, while the half-angle of the plume divergence is decreased from 39.2° to 35.5°. In addition, the rotating propellant increases the performance due to the continuous increase in the discharge voltage and anode flow rate. The graphs in Fig. 17a clearly illustrate the significant enhancement in the key parameters of the thruster with a rotational supply of krypton.

The three-dimensional maps of the ionization efficiency, peak-to-peak value of discharge current oscillations, and plume divergence half-angle for the thruster with rotational supply of krypton are shown in Figs. 17b and c [159]. The propellant rotation makes the ionization zone narrower, thus enhancing the ionization, and moves the ionization region upstream of the discharge channel. The measured flow rate-ampere characteristics confirmed the reduction of the ionization zone by a factor 1.1–1.2, an increase of the ionization rate by 1.4 times, and a shift of the ionization peak 2 mm upstream of the channel when comparing the thruster performance with the propellant rotation and axial supply modes at 300 V of the discharge power. The experiments reveal the mechanism of how the rotating propellant supply improves the ionization in the krypton-operated Hall thrusters. Moreover, the mode expands the range of a stable operation of the thrusters with respect to the applied strength of the magnetic field and discharge voltage.

5.4. *Damping instabilities in hollow cathodes by gas injection*

Control of gas supply is also useful for damping plasma instabilities in powerful hollow cathodes. The supply of additional neutral gas could reduce the instabilities in the hollow cathodes, which are a very important part of several types of the most used ion thrusters, including gridded ion and Hall systems. Fig. 18a illustrates the design of the cathode with such type of instability damping [120]. Gas is injected in the 2-cm-diameter LaB_6 X3 cathode operating at 200–350 A of discharge current. To date, the injection of extra neutral gas in the near cathode plume has been the only demonstrated successful method of damping both the ionization and ion-acoustic instabilities. Gas flows injected externally to the cathode orifice, and into the space between the keeper tubes and cathode, were applied according to the schematic shown in Fig. 18 with the purpose of damping the instabilities in the discharge current range of 200–350 A.

6. Narrow channel and capillary discharge thrusters

A tendency for miniaturization of space assets and thrusters that power them leads to the problem with discharge efficiency in low-dimension channels. This raised a strong interest in studies of the physics of discharges in narrow channels. When the narrow channels are properly designed and optimized, the discharge in them could be quite efficient [160]. Moreover, the capillary discharge could be used in the capacity of capillary discharge-based plasma thrusters [161]. The miniaturized hollow cathodes which also feature discharge in narrow channels and confined spaces, could also serve as the thrusters [162]. Below we will briefly outline several most recent ideas and results on the investigation of plasma discharges in confinement conditions.

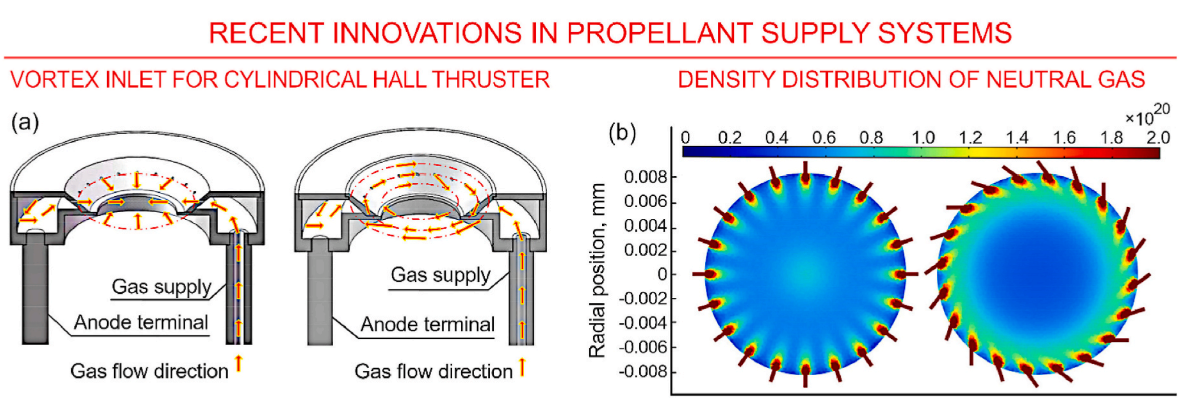

Fig. 16. Innovations in propellant supply systems. (a) Gas flow direction in low-power cylindrical Hall thruster (left: radial inlet mode and right: vortex inlet mode), (b) Density distribution of neutral gas in the cross-section of the propel-lant outlet. The vortex inlet mode features mode uniform density distribution. Reprinted with permission from Ding *et al.*, Phys. Plasmas 24, 080703 (2017).

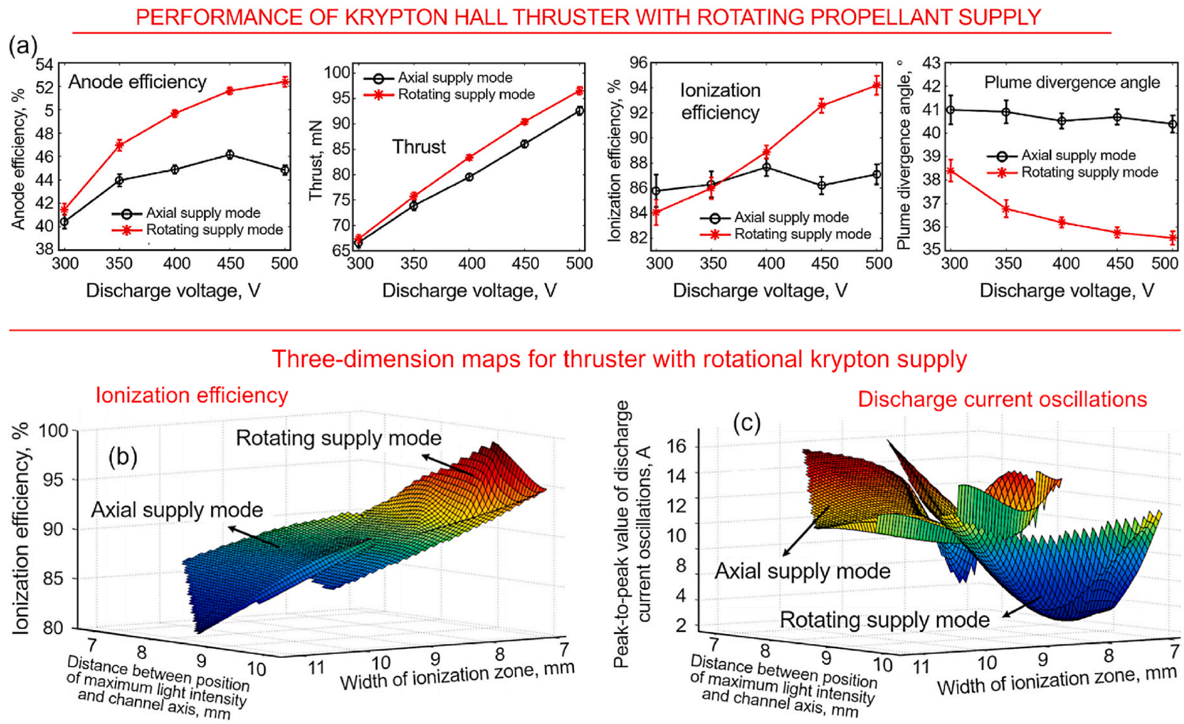

Fig. 17. Innovations in propellant supply systems. (a) Characteristics of the optimized Hall thruster with vertex-type propellant supply. The graphs clearly illustrate the significant enhancement in the key parameters of the thruster with rotational supply of krypton. Reprinted with permission from Xia *et al.*, Acta Astronaut. 171, 290–299 (**2020**). (b,c) Three-dimension maps of the ionization efficiency, peak-to-peak value of discharge current oscillations, and plume divergence half angle for the thruster with rotational supply of krypton. Reprinted with permission from Xia *et al.*, Vacuum 181, 109664 (**2020**).

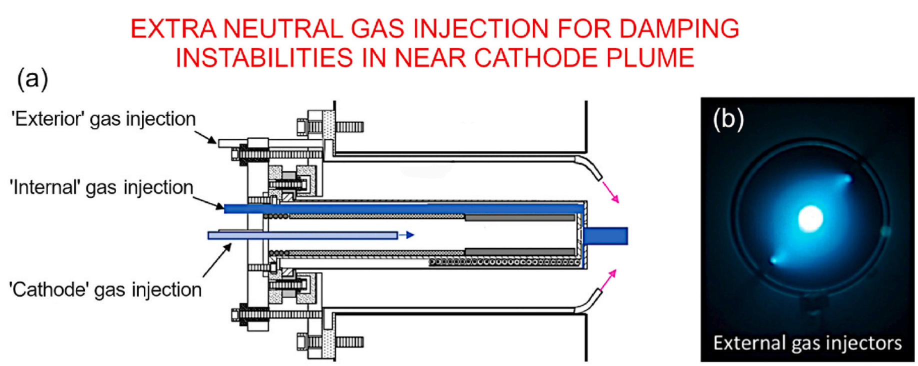

Fig. 18. Damping instabilities in hollow cathodes by gas injection. (a) Scheme of extra gas supply into hollow cathode to damp the instabilities in plasma, and (b) photograph of the discharge. Reprinted with permission from Goebel *et al.*, J. Appl. Phys. 130, 050902 (**2021**).

6.1. Narrow channel Hall thrusters

Currently, there are very few low-power Hall thrusters that can operate at power levels below 30–50 W. Recently, Hamo and Kronhaus described the characteristics of the narrow channel Hall thruster discharge [157]. Currently, Hall thrusters are developed to operate at powers lower than 100 W. In particular, a miniaturized Hall thruster with a narrow channel (NCHT) [163] can operate at the power of 15–30 W and a thrust-to-power ratio of approximately 50 μN/W, recently developed at the Aerospace Plasma Laboratory, Technion. While it preserves a general design of Hall thrusters, some unique improvements are introduced to enhance the ionization efficiency at the low power [164,165]. The densities of ions and ion current reach their peaks in the plume, which is conditioned by the distribution of the electrical potential drop that mostly occurs outside the discharge channel, as was measured in the experiment. The peak values found in the plume are as high as 10 eV for the electron temperature, 480 A/m^2 for the ion current density, and 1.2×10^{18} m^{-3} for the ion density. At the same time, the loss of ions on the walls of the discharge channel is still the main problem that should be solved in future models of NCHTs. Figs. 19a–c illustrates the design of the NCHT (a), a photograph of a 3 cm NCHT in operation (b) with the operating hollow cathode seen outside, and (c) the results of experimental measurements of the ion density outside the channel. The authors made a conclusion about the spatial separation of functions it the thruster, when plasma is generated in the channel, and is accelerated outside of it. This important finding contributes to the further works on the thrusters with the out-channel mechanisms of plasma acceleration, which is essential for decreasing wall wear and thus prolonging the thruster service life, urgently required for the nanosatellite-based scientific missions and probes.

6.2. Capillary discharge thrusters

Wang *et al.* have recently presented the capillary discharge-based

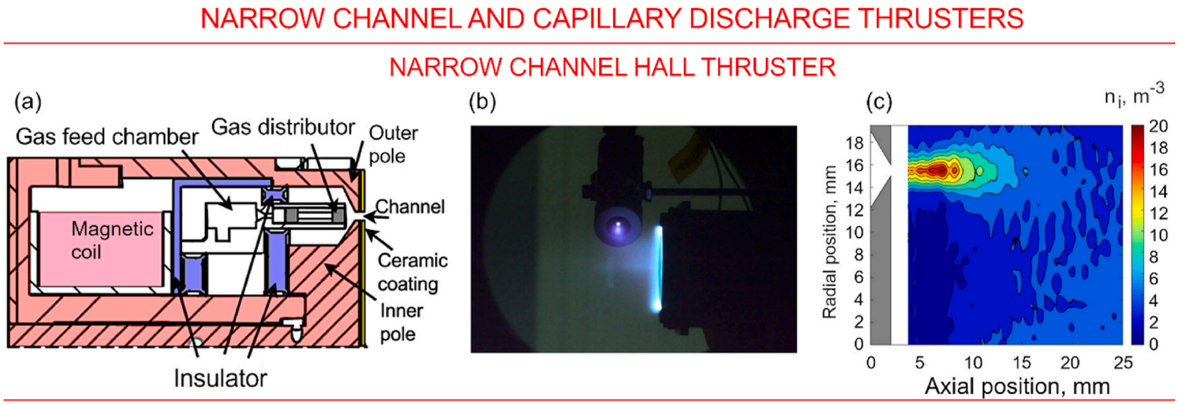

Fig. 19. Narrow channel thruster. (a–c) Narrow Channel Hall Thruster (NCHT). (a) The top half cross section of the NCHT. (b) A photograph of a 3-cm NCHT in operation. The hollow cathode is seen outside. (c) Experimental 2D measurements of the ion number density. Reprinted with permission from Hamo *et al.*, J. Appl. Phys. 130, 223301 (**2021**).

pulsed plasma thruster [158,166]. In comparison with other systems intended for electric propulsion, pulsed plasma thrusters have a wider range of parameters that can be adjusted by the application of different input powers and configurations, which increases their flexibility with respect to their implementation in micro- and nanosatellites. The capillary discharge based pulsed thruster is in fact a type of electrothermal thrusters and thus, it features a high thrust-to-power ratio, yet at very small dimensions. Fig. 20 illustrates the design, discharge, and characteristics of a novel capillary discharge thruster. In this system, the propellant ablation followed by the ionization utilizes the largest part of energy applied at the discharge ignition. As a result of the variation of pressure conditions in the channel, faster particles are accelerated early, and the slower particles – later in the pulse, while the neutrals are accelerated by a gas-dynamic force and the plasma equivalent velocity in a plume can be as high as 12.5–35 km/s. These are very promising results for the miniaturized thruster with the pulse discharge energy in the range of 1–10 J. Further developments of similar systems should be expected, with clear prospects for utilizing them on nano-satellites.

A miniature capacitively coupled radio frequency thruster with a capillary tube (C^3RFT) is being developed and tested at the Technion [167,168]. The thruster utilizes a nonsymmetric electrode arrangement and a dedicated radio frequency generator. The small diameter of the dielectric tube, 0.8 mm, allows operation of the device at very low flow rates, less than 8 sccm Ar [164]. The measured thrust time response and wall temperature of 400 °C confirm an electrothermal mechanism of thrust generation. At a constant input power, the thrust is shown to increase linearly with the flow rate. At an input power of 14 W and a flow rate of 8 sccm, the thrust increases significantly compared to the cold flow case, for a total thrust of approximately 160 μN and specific impulse of approximately 69 s on argon. When powering the larger inlet "back" electrode, discharge is observed to diverge from the classical theory of asymmetric capacitive coupled plasma, leading to mode transition. This phenomenon is marked by the appearance of bright plasma exhaust and a reduction in input power from approximately 15 W–∼9 W. The thrust-to-power ratio increased by 25% after the transition. A simple sheath breakdown model was proposed to explain the transition.

Concepts of hollow cathode thrusters. Fig. 21a shows the schemes of three conceptual variants of *hollow cathode thruster* developed at the Technische Universität Dresden, Germany. It should be noted that the thruster was developed as a spin-off project of a hollow cathode device. Different configurations are developed for the mN-thrusters based on the utilization of the materials with low work function, like C12A7, LaB_6, and thoriated tungsten. In the electrothermal design the thrust is generated by a heated propellant expanded and accelerated in nozzle. The preliminary tests confirmed the thrust was *higher than for the cold gas application*, yet it was accompanied by the lower thrust efficiencies. In the novel electromagnetic thruster, the applied magnetic field is directed orthogonally with respect to the discharge current, thus creating a system for the acceleration of the charged particles. In the case of C12A7 the tests were not successful; however, the modification that utilizes a thoriated tungsten wire proved the functionality of the concept. Fig. 21b shows the key parameters of the tested thrusters.

7. Outlook and perspectives

The heterogeneity of electric thrusters ideally allows for their use in any kind of mission, spanning the whole range of space vehicles and functions. Several promising concepts that are less mature with respect to the in-use propulsion systems are being explored and may be placed in operation in the near future.

7.1. Novel approaches

The ***photonic propulsion systems***, which use external or internal lasers to produce thrust, are now investigated to serve modern satellite systems and missions (Fig. 22). Different concepts of laser propulsion could have multiple applications, ranging from space micropropulsion systems to high-power thrusters with very high specific impulse. ***Magnetic reconnection,*** namely the conversion of field energy into energy of charged particles by a sharp change of the topology of a magnetic field, is a promising mechanism for space propulsion systems and acceleration of plasma, able to reach exhaust velocities and specific impulses comparable with the presently existing plasma thrusters. After simulations gave encouraging results, the development is now focused on the realization of a compact and energy-efficient prototype. ***Surface plasmon resonance*** is another mechanism to generate thrust in space, based on the acceleration of nanoparticles. Its envisaged application is mainly for attitude control of small satellites, possibly using a direct conversion of sunlight to thrust inside the thruster. Electroosmotic forces generated by electrostatic Coulombic forces could be exploited to expel electrolytic working liquids to the surrounding environment generating thrust, in the so-called ***kinetic/osmotic thrusters***. The implementation of this technology, demonstrated as lab-based prototypes of space thrusters, presents challenges in fabrication, materials, and thruster design; however, high efficiency and high thrust could be attained if successful solutions will be found. Matter acceleration by ***surface-acoustic waves*** (SAWs) could be potentially considered to efficiently generate low thrusts in space. Although the SAWs-based space thrusters have not yet been demonstrated, their implementation shall be feasible since the underlying processes are similar to osmotic thrusters.

The negative mass theory is one more promising direction for space

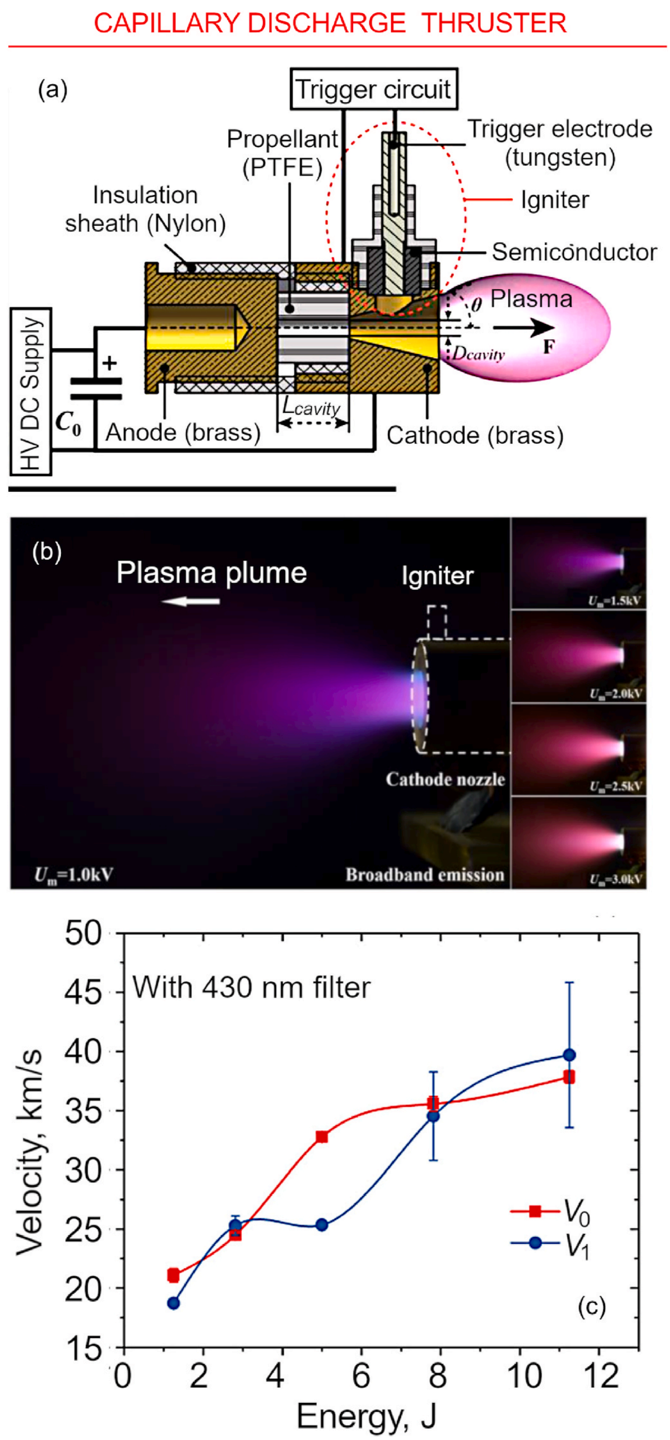

Fig. 20. Capillary discharge thruster. Design, discharge, and characteristics of a novel capillary discharge thruster. Reprinted with permission from Wang *et al.*, Phys. Plasmas 28, 123509 (**2021**).

propulsion. It is based on an analogy with electromagnetism, where negative and positive charges are distinguished; hence, it may be true for mass. Various assumptions are made with respect to the places where this kind of matter can be found [169]. Negative matter describes masses with gravitational, inertial and other properties opposite to the normal matter that operates with positive mass. It should be stressed that negative matter should not be confused with antimatter which is considered for now as dealing with positive mass. If an object with negative mass interacts with the same value of positive mass through gravitational, electromagnetic, or elastic forces, both the objects would be accelerated in the same direction without experiencing the necessity for a reaction mass or energy source. Despite the incredible properties, the negative propulsion does not violate *the Newtonian laws of energy and conservation of linear momentum*. Importantly, experimental evidence of a negative mass-like behavior has been recently reported [170]. Not surprisingly, this discovery has immediately attracted strong interest in media [171,172].

Concerning the matured space propulsion technologies, innovations being explored include enhancing the *active plasma control* in the EP thrusters, as well as the introduction of new control mechanisms and principles, with the aim of improving the performance and lifetime of space propulsion systems. Thrusters exploiting ***rotating magnetic field systems*** are close to implementation in miniaturized EP. Besides, rotational modes have been recently discovered in the plumes of high-current *hollow cathodes*, contributing to a deeper understanding of the physics of these devices and improving the possibility to design long-life electric thrusters. Another aspect in the spotlight of EP is the utilization of *alternative propellants* to xenon. Apart from krypton, which is presently supplying many Hall thrusters in space [173], iodine, bismuth, metals, and even water have been recently demonstrated as valid alternatives to inert gases. Innovations in *propellant supply systems* are also being investigated, with potential solutions to improve the thruster performance and damp plasma instabilities in hollow cathodes. ***Narrow channel and capillary discharge thrusters*** are of great interest in the frame of the miniaturization of space assets, offering valid solutions for micro-satellites and nano-satellites applications. ***Hollow cathode thrusters***, featuring discharge in narrow channels and confined spaces, are under study to produce millinewton thrust using thermionic electron emission from low work function materials.

Progress in diagnostics also could be an important factor for acceleration of a thruster's design and development. Here, automated test systems [174,175] and big data approaches capable of predicting the service life of thrusters designed for very long missions and affected by erosion [176,177] could be among the most critical achievements [178–180].

In addition to the above-mentioned novel technologies, other acceleration principles could be used to produce thrust in space and thus should be further investigated. For example, a pair of ***beating electrostatic waves*** was proposed to accelerate magnetized ions (so called "Coherent acceleration") [181]. For a single propagating electrostatic wave, an ion with a charge q and mass M_i can be accelerated when its velocity exceeds the value $V_{th} = \omega/k - \sqrt{qE/kM_i}$, where E, ω, and k are the amplitude of the electric field of the wave, frequency, and wave number. The ions with the velocities below the threshold value are considered as located in a regular (or coherent) region of phase space, while those with higher velocities are located in a stochastic region. For the two waves of frequencies ω_1 and ω_2 the acceleration occurs when ω_1 - $\omega_1 = n\omega_c$, where ω_c is the ion cyclotron frequency. In this case the regular and stochastic regions connect, thus allowing acceleration even the ions with the small velocities. Importantly, the appropriate set of initial conditions allows gaining significant energy for the particles [182,183].

Interesting concept was proposed recently by Kang *et al.* In the ***electrical supersonic thruster based on rotating gliding arc***, the arc discharge is ignited in a gap of 0.7 mm between a cone-shaped AC-biased (700–800 V, up to 10 A) electrode and the body of the discharge chamber, while CO_2 gas is supplied in swirling motion into the chamber to ensure the ignition [184]. The preliminary estimations were made for Martian atmosphere.

Another interesting technology is the ***interaction of helicon plasma with an expanding magnetic field*** which forms a current free double layer able to accelerate the plasma ions, as shown by Saini and Ganesh [185]. Basically, the pressure gradients and the confining magnetic field are responsible for the acceleration in a radial direction, while electrothermal (via expansion of heated gas) and electromagnetic

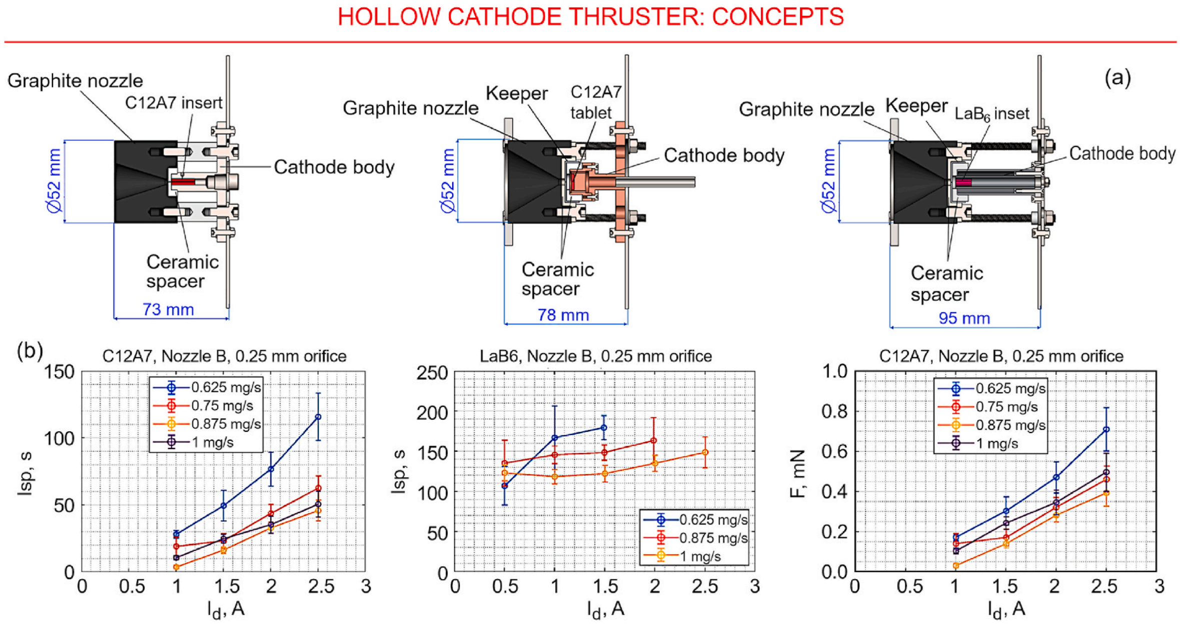

Fig. 21. Hollow cathode thruster. (a) Three conceptual variants and (b) the key characteristics of the hollow cathode thruster. Reprinted from Gondol *et al.*, CEAS Spae J. (**2021**) under terms and conditions of Creative Commons Attribution 4.0 International License.

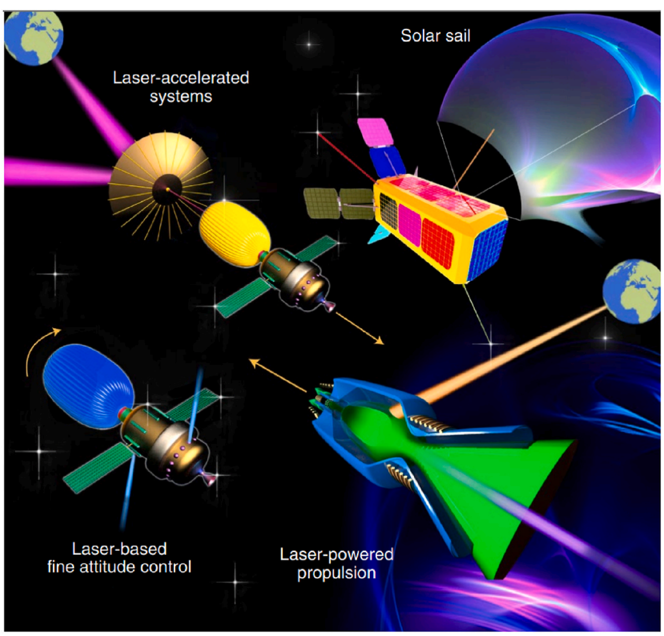

Fig. 22. Various types of photonic-based space thrust systems (artistic presentation). The laser-accelerated systems utilize external laser beams to generate the thrust via reflection. Solar sails use the radiation from the Sun, but produce lower thrust compared with laser-based propulsion system. Laser-enabled fine attitude controls use on-board- lasers to generate low thrust for precise attitude control of spacecraft. The laser-powered systems receive the energy from external lasers to accelerate propellant. Reprinted with permission from Nature Photon. 12, 649–657 (2018) [8].

(predominantly Hall mechanism via interaction of azimuthal current with the magnetic field $j_\Theta \times B_r$) acceleration are considered as the drivers in the axial direction. The measured profiles of an annular ion beam generated in the helicon thruster show a half-opening angle of about 30° and one-peak profile of the beam [186]. A thrust of about 1 mN was obtained for the magnetic field 0.01 T and the input power of about 500 W [187]. Radio frequency helicon thrusters with various nozzles is also a promising technology [80,188], along with the electron cyclotron resonance (ECR) plasma thrusters [189].

High-density helicon plasma sources were studied by Shinohara *et al.*, investigating the rotating magnetic field (RMF), ion cyclotron resonance/ponderomotive acceleration (ICR/PA), and rotating electric field (REF) schemes [190]. The RMF design implies a steady plasma current in toroidal configuration, which is guided in a steady-state noninductive manner by use of the rotating magnetic field and was initially developed also for fusion applications. The ICR/PA scheme uses a principle of ion parallel acceleration via the electromagnetic ***ponderomotive force***, which urges a charged particle to drift towards a domain of the weaker strength in an inhomogeneous oscillating electromagnetic field, when RF waves are applied to make the resonance point coinciding with the peak of the wave energy density. A numerical study has demonstrated that the ponderomotive acceleration is not as effective as the ion cyclotron resonance acceleration, at least for the parameters used in the model [191].

Helicon plasma with rotating electric field includes two facing electrodes mounted around a plasma vessel to create a rotating electric field in the presence of divergent magnetic field and thus to accelerate the plasma along the axis [192]. The same principle was studied by Nakamura *et al.* in the experimental research of plasma that is electromagnetically accelerated in a helicon thruster by use of a rotating electric field in the presence of a diverging static magnetic field [193]. It was found that the greatest increase of the velocity was due to the increase in the electron temperature.

7.2. Atmosphere-breathing electric propulsion systems

The atmosphere-breathing electric propulsion (ABEP) systems are a relatively novel propulsion platform that currently attracts strong interest from the researchers and engineers. This system allows thrust creation at very low Earth orbit (VLEO). Rarefied atmosphere is used in these systems in the capacity of propellant gas, without the need to launch it with the satellite, and to keep it ion-board. Collection and compression of atmospheric particles is made in this case with the intake devices. Apparently, the area of intake device determines the inflow of propellant from the atmosphere and thus influences the performance characteristics of the thrusters. Currently, a very limited number of satellites operate at VLEO, *i.e.,* at the attitudes of 250 km or below. On the other hand, the low Earth orbits offer great advantages for satellites, such as *e.g.,* lower launch costs, higher observation accuracy, less communication losses, safer operation environment, and many others. However, spacecraft at low orbits are affected by the atmosphere, yet rarefied, and the larger aerodynamic drag. Low gas pressure means a small amount of gas collected for the thrusters, so the thrust could be limited. Also, atomic oxygen could adversely affect the systems and cause erosion and oxidation of spacecraft and the thrusters. Fig. 23 illustrates the concept of ABEP system. Currently, various ABEP systems are under development, yet the flight tests dates have not been set [194–197].

Another thruster designed for space missions at very low altitudes employs the helicon-based inductive plasma. In a recent study several novel feature was used. Specifically, a cylindrical birdcage antenna similar to that used in the magnetic resonance imaging and fusion experiments ignited inductively coupled plasma in a region of a static magnetic field created by a solenoid wound around the antenna [198]. The interaction of the electromagnetic field generated by the antenna with the magnetic field of the solenoid results in the acceleration of helicon plasma.

7.3. Electrodynamic tethers and tether-enabled systems

Electrodynamic tethers (EDTs) are long wires able to conduct electrical current and perform as electromagnetic generators, when transforming their kinetic energy into electrical energy or otherwise. These wires can be deployed from a satellite, and the electric potential is generated when moving the structure through the magnetic field of a planet. Three main parts are distinguished in tethered satellites, such as a base satellite, a tether, and a sub-satellite. The first part (base satellite) contains the other two parts until deployment. A spacecraft, another satellite, or even the Moon can serve as the base-satellite. The tether serves as a connecting cable between the base- and sub-satellites. Usually, a spring ejection system is used to release the sub-satellite that is pushed further by gravity or centrifugal force.

Electrodynamic tether propulsion is based on thrust conditioned by Lorentz force that is generated when a current through the tether interacts with the magnetic field of a planet that is used as a reaction mass instead of expelled propellant. A lot of applications require such tethers, such as artificial gravity, momentum exchange, sensor positioning, to mention but a few. After the tether deployment, the station can be kept for some time, and then the system can be retracted if the deployment

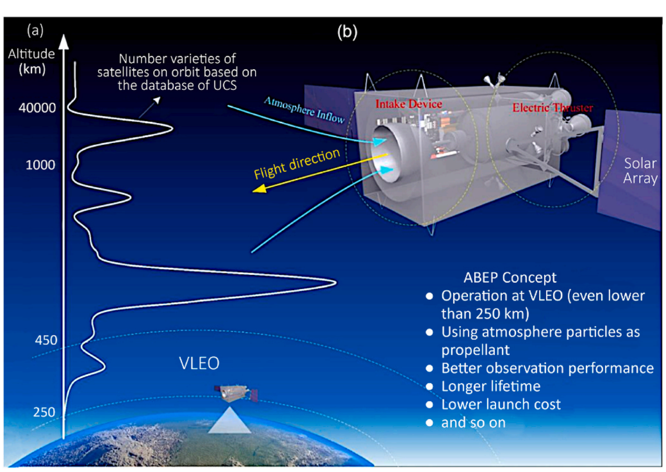

Fig. 23. Distribution of satellites over altitudes (a), based on the database of UCS; (b) ABEP concept using atmospheric particles as the propellant of electric thruster. Application of atmosphere breathing EP systems could help to utilize very low orbits, useful for many applications such as high-resolution observations. Reprinted from Wu *et al.*, J. Prog. Aerospace Sci. **2022**.

system is designed for the purpose.

Electrodynamic tethers: the first tests. Electrodynamic tethers were proposed several years ago, and currently, several orbital missions were accomplished by use of the electromagnetic tethers in space, *e.g.,* the experiments with Plasma Motor Generator (PMG), TSS-1, and TSS-1R. Fig. 24a shows the early biography of tether technology tests at low Earth orbits. The Tethered Satellite System-1 (TSS-1) was proposed by NASA and the Italian Space Agency (ASI), was flown in 1992, during STS-46 aboard the Space Shuttle Atlantis from 31 July to 8 August. The PROPEL (Propulsion using Electrodynamics) mission was proposed to demonstrate the operation of an electrodynamic tether propulsion system in low Earth orbit and advance its technology readiness level for multiple applications [199].

Apart from the orbital experiments, the tethered techniques were successfully tested using sounding rockets. Figs. 24b and c illustrate one of these experiments, the space demonstration of bare electrodynamic tape-tether technology on the sounding rocket S520-25 [200]. The ***T-Rex (Tether Rocket experiment)*** mission was launched aboard a S520-25 sounding rocket on 31 August 2010 by ISAS/JAXA from Uchinoura site to an altitude of 300 km (velocity about 0.5 km/s) and successfully deployed 132.6 m of tape tether over 120 s in a ballistic flight. The electrodynamic performance of the bare tape tether employed as an atmospheric probe was measured. The EDT was extended in the direction of flight to intersect at 45° the direction of the magnetic field of the Earth, which was confirmed by data from a magnetometer. The purpose of the experiment was to check the EDF performance in space with respect to the following characteristics: reliable deployment of long tethers; fast operation of hollow cathodes in supplying the electricity to the tether; use of EDT as a collector of electrons; verification of theories of the electron collection; check of the interaction of tape tether with atmosphere; check of a system of a robotized motions in space. A bare electrodynamic tether made of reinforced Al with a thickness of 0.05 mm and width of 25 mm was used in the experiments with a Langmuir tube, when the tether was extended for the full length to afford the necessary time of 5 min for the experiments in space. As a result, the successful application of T-Rex for most of the tasks was confirmed.

Electrodynamic tethers among other systems. Fig. 24d shows the place of electrodynamic tether technology among the other EP systems by comparison of specific impulse vs. thrust-to-power characteristics of ED tethers. Apparently, this technology holds very high promises featuring *efficient specific impulse of about* 10^5 *s* with very high thrust-to-power parameter, well exceeding that of *e.g.,* gridded ion and Hall thrusters. Note that while the tether system does not utilize any propellant gas (in fact, the tether system is not a reactive propulsion system, in contrast to any other type of propulsion thrusters), it still uses a ***plasma contactor*** device whose function is to ensure electric current between the tether and ambient ionosphere; in the capacity of such contactors, ***hollow cathodes*** are usually considered which require some flow of ***expellant*** (like hollow cathodes in the electric propulsion thrusters *e.g.,* Hall type). Plasma contactor generates plasma plume that ensures electrical contact between design parts of tether and ionosphere. As a result, a powerful tether system will still need some mass of expellant, yet much less than traditional EP thrusters. Solid expellant also can be used to simplify the design.

How powerful could be an EDT system? Fig. 24e shows the calculated variation of power generation capability with tether length. Importantly, *the power generation capability varies essentially linearly with the tether length* [201]. The order is 1 kW per 10 km of the tether length – that is, quite useable power levels could be achieved for realistic length (note that tethers of several km have already been tested in orbit). Fig. 24f shows the normalized averaged current in the tether as the function of a normalized length for various sets of dimensionless parameters, which depend on electron Debye length and electron temperature in space plasma, as well as on the tether characteristics including tether material temperature and conductivity, and

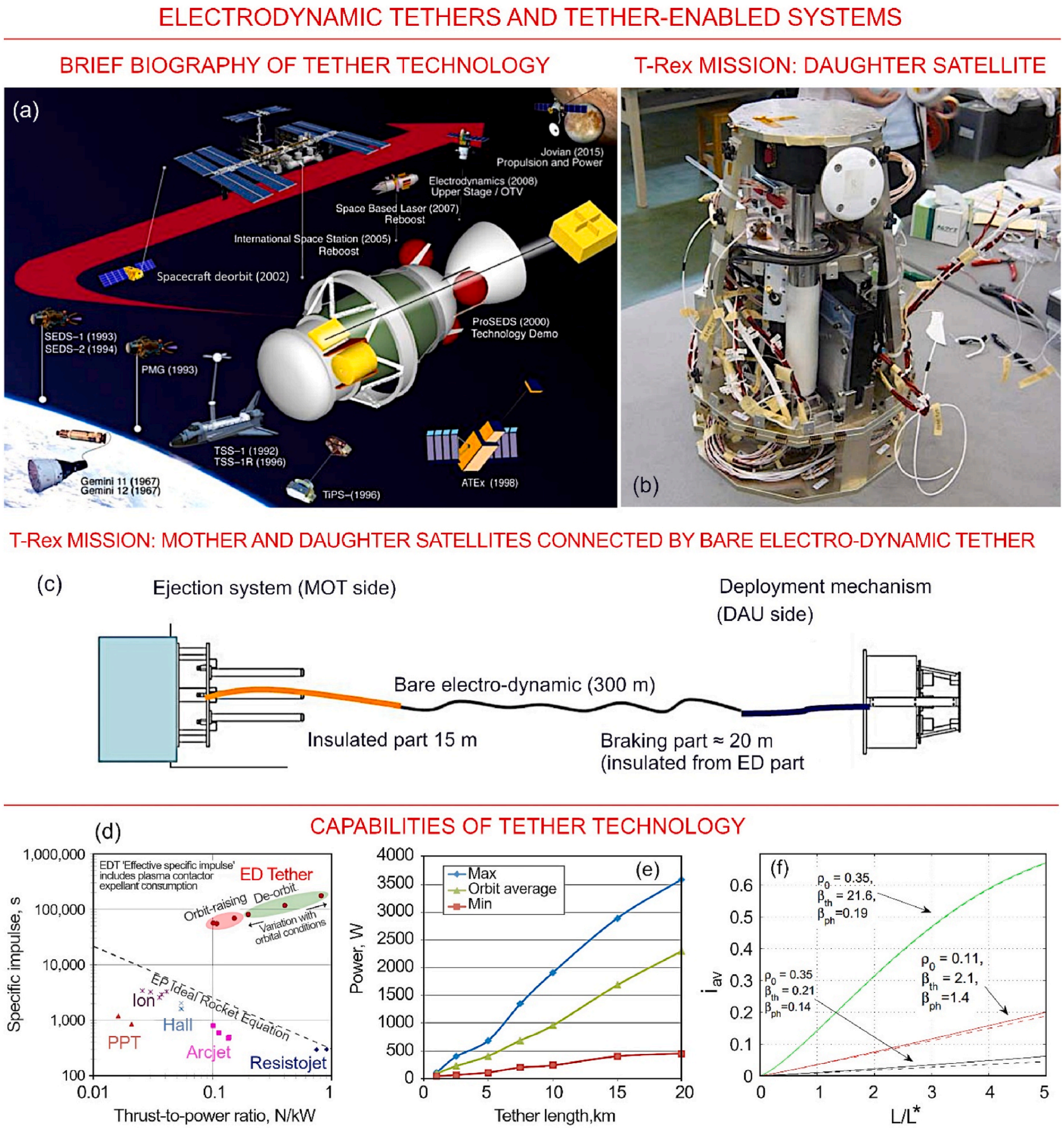

Fig. 24. Capabilities of space tether systems. (a) Short history of tether technology (b,c) Results of implementation of Bare Electrodynamic Tape-Tether Technology on the Sounding Rocket S520-25. (b) Daughter Satellite (DAU) and (c) Payload as Mother satellite (MOT) and DAU connected by bare EDT. Reprinted with permission from Fujii *et al.*, paper AIAA 2011–6503. Copyright AIAA. (d) Specific impulse vs. thrust-to-power characteristics of EDTs and EP technologies. Electrodynamic interactions with the geomagnetic field do not imply the use of propellant, thus allowing to overcome the limitations of the rocket equation to increase as I_{sp} as EP thrust. (e) Calculated function of the power generation depends linearly on the length of tether. Reprinted with permission from Hoyt *et al.*, paper AIAA 2011–7321. (f) Normalized averaged current in the tether as the function of a normalized length for various sets of dimensionless parameters. Reprinted with permission from Sanchez-Arriaga *et al.*, J. Propuls. Power 34, 213–220 (2018).

tether-to-plasma bias.

The physics of the tether-to-plasma interaction is complex, and not surprisingly, several detailed models were recently developed. In the EDT circuit where hollow cathode plasma contactors (HCPCs) are intended to serve as the electron emitters as the electron collectors, the impedance of the collection is a dominant factor affecting the power generation and the system efficiency. Unfortunately, EDF performance cannot be predicted with the necessary precision due to the problematic issues in the description of the processes of the electron collection. Up to now, two theoretical models have been developed to describe the upper and lower limits of the collection performance. Katz *et al.* [202] assume that plasma plume in HCPC's distribution is close to spherical, and the radius of the plume depends on the ion current across the spherical surface of the plume. Gerver *et al.* [203] suggest a cylindrical geometry along the lines of the Earth's magnetic field, which predicts the higher collected currents at a fixed ion current and bias voltage.

7.4. Novel materials and material systems

The materials-based progress in space propulsion systems is out of the scope of our review, so we will only mention several recent trends in the application of novel materials and technologies for advanced space propulsion systems. Integration of novel advanced materials could be a factor of significant enhancement of the operational characteristics of electric propulsion systems [204,205]. Metamaterials [206–209] and functional metamaterial-based architectures are among the most attractive materials platform that could potentially bring a very significant advance for the space propulsion technology [210,211]. Advanced materials for heat exchange and heat insulation also could significantly enhance thrusters characteristics [212,213]. Materials for future tethered systems are currently also under careful consideration, in view of a strong interest in the dynamics and application of tether systems [214]. Advanced technologies for manufacturing space propulsion systems include 3D printing [215–217], laser sintering, and plasma-based methods [218] that allow fabrication of complex metamaterials with unique properties. Novel materials for efficient on-board power systems include nanomaterial-based supercapacitors [219–223], advanced polymers [224], and super-hydrophilic and super-hydrophobic materials [225].

8. Concluding remarks

In this paper we outlined the most recent (mainly published in 2019–2022) and most important novel physical mechanisms, innovations, concepts, and discoveries that could potentially boost both matured and future space propulsion technologies. Among others, we discussed the recent advances in active plasma control in electric thruster systems such as *e.g.,* additional magnetic coils and electrodes, segmented electrodes and other techniques, and stages thrusters; recent advances in rotating magnetic field systems including Rotamak-type systems and helicon antenna-based plasma sources; innovations in alternative propellants and propellant supply systems including condensable propellant thrusters; and innovations in propellant supply systems, narrow channel and capillary discharge thrusters. The main aim was to promote the most recent innovations for the future consolidated research efforts worldwide, and to finally help enhance the key parameters of space propulsion systems for future ambitious missions and ultimately, to contribute to the creation of substantially novel thrust platforms for the new era of space exploration.

Declaration of competing interest

The authors declare that they have no known competing financial interests or personal relationships that could have appeared to influence the work reported in this paper.

Data availability

No data was used for the research described in the article.

Acknowledgments

This work was supported in part by the following funds and organizations: OSTIn-SRP/EDB through National Research Foundation and in part by MoE AcRF (Rp6/16 Xs), Singapore; I.L. acknowledges the support from the National Institute of Education, Nanyang Technological University of Technology; special thanks to the entire Plasma Sources and Application Centre/Space Propulsion Centre, Singapore for their help; O.B. acknowledges the support from the National Research Foundation of Ukraine under grant agreement No. 2020.02/0119, and the NATO Science for Peace and Security Programme under grant id. G5814 project NOOSE. K.B. acknowledges the funding from the Australian Research Council Future Fellowship (FT190100819), the Australian National University Futures Scheme, and New South Wales Space Research Network Research Pilot program.

References

[1] E. Musk, Making Humans a multi-planetary species, New Space 5 (2017) 46–61, https://doi.org/10.1089/space.2017.29009.emu.
[2] S. Do, A. Owens, K. Ho, S. Schreiner, O. deWeck, An independent assessment of the technical feasibility of the mars one mission plan – updated analysis, Acta Astronaut. 120 (2016) 192–228, https://doi.org/10.1016/j.actaastro.2015.11.025.
[3] I. Levchenko, S. Xu, S. Mazouffre, M. Keidar, K. Bazaka, Mars colonization: beyond Getting there, Global Challenges 2 (2018) 1800062, https://doi.org/10.1002/gch2.201800062.
[4] I. Levchenko, M. Keidar, J. Cantrell, Y.-L. Wu, H. Kuninaka, K. Bazaka, S. Xu, Explore space using swarms of tiny satellites, Nature 562 (2018) 185, https://doi.org/10.1038/d41586-018-06957-2.
[5] I. Levchenko, K. Bazaka, Y. Ding, Y. Raitses, S. Mazouffre, T. Henning, P.J. Klar, S. Shinohara, J. Schein, L. Garrigues, M. Kim, D. Lev, F. Taccogna, R.W. Boswell, C. Charles, H. Koizumi, S. Yan, C. Scharlemann, M. Keidar, S. Xu, Space micropropulsion systems for Cubesats and small satellites: from proximate targets to furthermost frontiers, Appl. Phys. Rev. 5 (2018) 011104, https://doi.org/10.1063/1.5007734.
[6] N. Kishi, Management analysis for the space industry, Space Pol. 39–40 (2017) 1–6, https://doi.org/10.1016/j.spacepol.2017.03.006.
[7] I. Levchenko, S. Xu, S. Mazouffre, D. Lev, D. Pedrini, D. Goebel, L. Garrigues, F. Taccogna, K. Bazaka, Perspectives, frontiers, and new horizons for plasma-based space electric propulsion, Phys. Plasmas 27 (2020) 020601, https://doi.org/10.1063/1.5109141.
[8] I. Levchenko, K. Bazaka, S. Mazouffre, S. Xu, Prospects and physical mechanisms for photonic space propulsion, Nat. Photonics 12 (2018) 649–657, https://doi.org/10.1038/s41566-018-0280-7.
[9] B. Beaurepaire, A. Vernier, M. Bocoum, F. Böhle, A. Jullien, J.-P. Rousseau, T. Lefrou, D. Douillet, G. Iaquaniello, R. Lopez-Martens, A. Lifschitz, J. Faure, Effect of the laser wave front in a laser-plasma accelerator, Phys. Rev. X 5 (2015) 031012, https://doi.org/10.1103/PhysRevX.5.031012.
[10] K. Lemmer, Propulsion for CubeSats, Acta Astronaut. 134 (2017) 231–243, https://doi.org/10.1016/j.actaastro.2017.01.048.
[11] I. Levchenko, S. Xu, Y.L. Wu, K. Bazaka, Hopes and concerns for astronomy of satellite constellations, Nat. Astron. 4 (2020) 1012–1014, https://doi.org/10.1038/s41550-020-1141-0.
[12] I. Adamovich, S.D. Baalrud, A. Bogaerts, P.J. Bruggeman, M. Cappelli, V. Colombo, U. Czarnetzki, U. Ebert, J.G. Eden, P. Favia, D.B. Graves, S. Hamaguchi, G. Hieftje, M. Hori, I.D. Kaganovich, U. Kortshagen, M.J. Kushner, N.J. Mason, S. Mazouffre, S.M. Thagard, H.-R. Metelmann, A. Mizuno, E. Moreau, A.B. Murphy, B.A. Niemira, G.S. Oehrlein, Z.L. Petrovic, L.C. Pitchford, Y.-K. Pu, S. Rauf, O. Sakai, S. Samukawa, S. Starikovskaia, J. Tennyson, K. Terashima, M. M. Turner, M.C.M. van de Sanden, A. VardelleHide, The 2017 Plasma Roadmap: low temperature plasma science and technology, J. Phys. D Appl. Phys. 50 (2017) 323001.
[13] L. Dubois, F. Gaboriau, L. Liard, D. Harribey, C. Henaux, L. Garrigues, G.J. H. Hagelaar, S. Mazouffre, C. Boniface, J.P. Boeuf, A new double stage Hall thruster design. I. Principle and hybrid model of ID-HALL, Phys. Plasmas 25 (2018) 093503.
[14] K. Takase, K. Takahashi, Y. Takao, Effects of neutral distribution and external magnetic field on plasma momentum in electrodeless plasma thrusters, Phys. Plasmas 25 (2018) 023507.
[15] N. Tiwari, S. Bhandari, S. Ghorui, Stability and structures in atmospheric pressure DC non-transferred arc plasma jets of argon, nitrogen, and air, Phys. Plasmas 25 (2018) 072103.
[16] T. Furzukawa, K. Shimura, D. Kuwahara, S. Shinohara, Verification of azimuthal current generation employing a rotating magnetic field plasma acceleration method in an open magnetic field configuration, Phys. Plasmas 26 (2019) 033505.
[17] J. Tian, Wenzheng Liu, Y. Gao, L. Zhao, Discharge and metallic plasma generation characteristics of an insulated anode with a micropore, Phys. Plasmas 26 (2019) 023511.
[18] L. Cheng, Y. Wang, W. Ding, C. Ge, J. Yan, Y. Li, Z. Li, A. Sun, Experimental study on the discharge ignition in a capillary discharge based pulsed plasma thruster, Phys. Plasmas 25 (2018) 093512.
[19] C. Charles, Plasmas for spacecraft propulsion, J. Phys. D Appl. Phys. 42 (2009) 163001.
[20] S. Mazouffre, Electric propulsion for satellites and spacecraft: established technologies and novel approaches, Plasma Sources Sci. Technol. 25 (2016) 033002.
[21] K. Nakagawa, T. Tsuchiya, Y. Takao, Microfabricated emitter array for an ionic liquid electrospray thruster, Jpn. J. Appl. Phys. 56 (2017) 06GN18.
[22] R.W. Conversano, D.M. Goebel, I.G. Mikellides, R.R. Hofer, Performance analysis of a low-power magnetically shielded Hall thruster: computational modeling, J. Propul. Power 33 (2017) 992–1001.
[23] Y. Ding, H. Su, P. Li, L. Wei, H. Li, W. Peng, Y. Xu, H. Sun, D. Yu, Study of the catastrophic Discharge phenomenon in a Hall thruster, Phys. Lett. 381 (2017) 3482–3486.
[24] K. Holste, et al., Ion thrusters for electric propulsion: scientific issues developing a niche technology into a game changer, Rev. Sci. Instrum. 91 (2020) 061101, https://doi.org/10.1063/5.0010134.
[25] Voyager 1 Fires up Thrusters after 37 Years, 2018.
[26] Y. Ding, L. Wang, H. Fan, H. Li, W. Xu, L. Wei, P. Li, D. Yu, Simulation research on magnetic pole erosion of Hall thrusters, Phys. Plasmas 26 (2019) 023520.
[27] I. Levchenko, O. Baranov, J. Fang, O. Cherkun, S. Xu, K. Bazaka, Focusing plasma jets to achieve high current density: feasibility and opportunities for applications in debris removal and space exploration, Aero. Sci. Technol. 108 (2021) 106343, https://doi.org/10.1016/j.ast.2020.106343.

[28] J.L. Rovey, C.T. Lyne, A.J. Mundahl, N. Rasmont, M.S. Glascock, M. J. Wainwright, S.P. Berg, Review of multimode space propulsion, Prog. Aero. Sci. 118 (2020) 100627.
[29] NASA's OSIRIS-REx successfully stows sample of asteroid Bennu. https://www.nasa.gov/press-release/nasa-s-osiris-rex-successfully-stows-sample-of-asteroid-bennu. Accessed January 2021.
[30] D.S. Lauretta, et al., The unexpected surface of asteroid (101955) Bennu, Nature 568 (2019) 55–60, https://doi.org/10.1038/s41586-019-1033-6.
[31] D.S. Lauretta, OSIRIS-REx asteroid sample-return mission, in: J. Pelton, F. Allahdadi (Eds.), Handbook of Cosmic Hazards and Planetary Defense, Springer, Cham, 2015, https://doi.org/10.1007/978-3-319-03952-7_44.
[32] Asteroid Explorer, Hayabusa2. http://www.hayabusa2.jaxa.jp/en (Accessed: January 2021).
[33] K. Wada, M. Grott, P. Michel, et al., Asteroid Ryugu before the Hayabusa2 encounter, Prog. Earth Planet. Sci. 5 (2018) 82, https://doi.org/10.1186/s40645-018-0237-y.
[34] S. Shinohara, Helicon high-density plasma sources: physics and applications, Adv. Phys. X 3 (2018) 1420424.
[35] S. Shinohara, H. Nishida, T. Tanikawa, T. Hada, I. Funaki, K.P. Shamrai, Development of electrodeless plasma thrusters with high-density helicon plasma sources, IEEE Trans. Plasma Sci. 42 (2014) 1245–1254.
[36] E. Gibney, How to build a MOON base, Nature 562 (2018) 474–478, https://doi.org/10.1038/d41586-018-07107-4.
[37] J.C. McDowell, The low Earth orbit satellite population and impacts of the SpaceX Starlink constellation, Astrophys. J. Lett. 892 (2020) L36, https://doi.org/10.3847/2041-8213/ab8016.
[38] Starlink. https://www.starlink.com, 2022. Accessed May.
[39] J.C. McDowell, The low earth orbit satellite population and impacts of the SpaceX Starlink constellation. https://arxiv.org/pdf/2003.07446.pdf, 2020.
[40] B. Imaz-Lueje, D.R. Prado, M. Arrebola, M.R. Pino, Reflect array antennas: a smart solution for new generation satellite mega-constellations in space communications, Sci. Rep. 10 (2020) 21554, https://doi.org/10.1038/s41598-020-78501-0.
[41] P. Kroupa, I. Banik, H. Haghi, A.H. Zonoozi, Jörg Dabringhausen, B. Javanmardi, O. Müller, X. Wu, H. Zhao, A common Milgromian acceleration scale in nature, Nat. Astron. 2 (2018) 925–926, https://doi.org/10.1038/s41550-018-0622-x.
[42] M. Armano, H. Audley, J. Baird, P. Binetruy, M. Born, D. Bortoluzzi, E. Castelli, A. Cavalleri, A. Cesarini, A.M. Cruise, et al., Beyond the required LISA free-fall performance: new LISA pathfinder results down to 20 μHz, Phys. Rev. Lett. 120 (2018) 061101, https://doi.org/10.1103/PhysRevLett.120.061101.
[43] The laser interferometer space antenna (LISA) mission. https://sci.esa.int/web/lisa, 2021. Accessed January.
[44] W.-R. Hu, Y.-L. Wu, The Taiji program in space for gravitational wave physics and the nature of gravity, Natl. Sci. Rev. 4 (2017) 685–686, https://doi.org/10.1093/nsr/nwx116.
[45] K. Abich, A. Abramovici, B. Amparan, A. Baatzsch, B.B. Okihiro, D.C. Barr, M. P. Bize, C. Bogan, C. Braxmaier, M.J. Burke, et al., In orbit performance of the GRACE follow-on laser ranging interferometer, Phys. Rev. Lett. 123 (2019) 031101. https://journals.aps.org/prl/abstract/10.1103/PhysRevLett.123.031101.
[46] J.D. Liddle, A.P. Holt, S.J. Jason, K.A. O'Donnell, E.J. Stevens, Space science with CubeSats and nanosatellites, Nat. Astron. 4 (2020) 1026–1030, https://doi.org/10.1038/s41550-020-01247-2.
[47] E.L. Shkolnik, On the verge of an astronomy CubeSat revolution, Nat. Astron. 2 (2018) 374–378, https://doi.org/10.1038/s41550-018-0438-8.
[48] D. Schulze-Makuch, W. Bains, Time to consider search strategies for complex life on exoplanets, Nat. Astron. 2 (2018) 432–433, https://doi.org/10.1038/s41550-018-0476-2.
[49] P. Schattschneider, A.A. Jackson, The Fishback ramjet revisited, Acta Astronaut. 191 (2022) 227–234, https://doi.org/10.1016/j.actaastro.2021.10.039.
[50] L. Johnson, M. Meyer, B. Palaszewski, D. Coote, D. Goebel, H. White, Development priorities for in-space propulsion technologies, Acta Astronaut. 82 (2013) 148–152, https://doi.org/10.1016/j.actaastro.2012.05.006.
[51] M. Wu, C. Xiao, X. Wang, C. Tan, T. Xu, R. He, R. Yuan, A. Xu, A new configuration for high power propulsion plasmas driven by ion cyclotron resonance energization, Phys. Plasmas 29 (2022) 023508, https://doi.org/10.1063/5.0073439.
[52] D.M. Goebel, I. Katz, Fundamentals of Electric Propulsion: Ion and Hall Thrusters, John Wiley & Sons, 2008.
[53] K. Takahashi, Y. Takao, A. Ando, Increased thrust-to-power ratio of a stepped-diameter helicon plasma thruster with krypton propellant, J. Propul. Power 36 (2020) 961, https://doi.org/10.2514/1.B37940.
[54] R.G. Jahn, Physics of Electric Propulsion, Dover Books on Physics. Dover Publications, 2006, ISBN 0486450406.
[55] H. Tahara, Y. Kagaya, T. Yoshikawa, Hybrid MPD thruster with axial and cusp magnetic fields, in: Presented at the 26th International Electric Propulsion Conference, IEPC-88-058, Garmisch-Partenkirchen, W. Germany, October .
[56] R. Albertoni, P. Rossetti, F. Paganucci, M. Andrenucci, M. Zuin, E. Martinez, R. Cavazzana, Experimental study of a 100-kW class applied-field MPD thruster, in: Presented at the 32nd International Electric Propulsion Conference, EPC-2011-110, Wiesbaden, Germany, 2011.
[57] V.B. Tikhonov, S.A. Semenikhin, J.R. Brophy, J.E. Polk, Performance of the 130 kW MPD thruster with an external magnetic field and Li as propellant, in: Presented at the 25th International Electric Propulsion Conference, IEPC-97-117, Cleveland, OH USA, 1997.
[58] F. Paganucci, P. Rossetti, M. Andrenucci, V.B. Tikhonov, V.A. Obukhov, Performance of an applied field MPD thruster, in: Presented at the 27th International Electric Propulsion Conference, IEPC-01-132, Pasadena, CA USA, 2001.
[59] G. Herdrich, U. Bauder, A. Boxberger, R.A. Gabrielli, M. Lau, D. Petkow, M. Pfeiffer, C. Syring, S. Fasoulas, Advanced plasma (propulsion) concepts at IRS, Vacuum 88 (2013) 36–41, https://doi.org/10.1016/j.vacuum.2012.02.032.
[60] J.W.M. Lim, I. Levchenko, S. Huang, L. Xu, R.Z.W. Sim, J.S. Yee, G.C. Potrivitu, Y. Sun, K. Bazaka, X. Wen, J. Gao, S. Xu, Plasma parameters and discharge characteristics of lab-based krypton-propelled miniaturized Hall thruster, Plasma Sourc. Sci. Technol. Technol. 28 (2019) 064003, https://doi.org/10.1088/1361-6595/ab07db.
[61] A.E. Vincia, S. Mazouffre, Direct experimental comparison of krypton and xenon discharge properties in the magnetic nozzle of a helicon plasma source, Phys. Plasmas 28 (2021) 033504, https://doi.org/10.1063/5.0037117.
[62] J. Sazbo, Electric Propulsion Research Accelerates toward the Future, Aerospace America, 2021.
[63] J. Vaudolon, V. Vial, N. Cornu, I. Habbassi, PPSR© X00 thruster development status at safran, in: Proc. 36th Int. Electric Prop. Conf., 2019. Vienna, Austria.
[64] L.L. Su, B.A. Jorns, Performance comparison of a 9-kW magnetically shielded Hall thruster operating on xenon and krypton, J. Appl. Phys. 130 (2021) 163306, https://doi.org/10.1063/5.0066849.
[65] A. Piragino, F. Faraji, M. Reza, E. Ferrato, A. Piraino, T. Andreussi, Background pressure effects on the performance of a 20 kW magnetically shielded Hall thruster operating in various configurations, Aerospace 8 (2021) 69, https://doi.org/10.3390/aerospace8030069.
[66] J. Simmonds, Y. Raitses, Ion acceleration in a wall-less Hall thruster, J. Appl. Phys. 130 (2021) 093302, https://doi.org/10.1063/5.0062607.
[67] R.W. Conversano, R.B. Lobbia, A.L. Ortega, V.H. Chaplin, S. Arestie, D.M. Goebel, Long-duration wear testing of the ASTRAEUS thruster, Phase II: 20 kg Xe Throughput at 500 V - 1000 W, AIAA Propulsion Energy Forum (2021), https://doi.org/10.2514/6.2021-3443.
[68] Scott J. Hall, Benjamin A. Jorns, Sarah E. Cusson, Alec D. Gallimore, Hani Kamhawi, Peter Y. Peterson, Thomas W. Haag, Jonathan A. Mackey, Matthew J. Baird, James H. Gilland, Performance and high-speed characterization of a 100-kW nested Hall thruster, AIAA Propulsion Energy Forum (2021), https://doi.org/10.2514/1.B38080 (VIRTUAL EVENT).
[69] Y. Kim, D. Lee, G. Doh, J. Park, W. Choe, Performance comparison of xenon and krypton discharges in a 300 W-class Hall thruster, in: Presented at the 37th International Electric Propulsion Conference, Massachusetts Institute of Technology, Cambridge, MA USA, 2022. IEPC-2022-336.
[70] B. Wang, H. Tang, Y. Wang, C. Lu, C. Zhou, Y. Dong, G. Wang, Y. Cong, D. Luu, J. Cao, A 100 KW class applied-field magnetoplasmadynamic thruster, J. Vis. Exp. 142 (2018) 58510.
[71] H. Yao, W. Yang, T. Zhang, B. Wang, H. Tang, Electromagnetic properties analysis on superconducting magnet coil for magnetoplasmadymamic thrusters, Chin. Space Sci. Technol. 37 (2017) 1–8.
[72] W.J. Coogan, M.A. Hepler, E.Y. Choueiri, Method for measuring the applied-field thrust component of plasma thrusters, J. Propul. Power 34 (2018) 1609, https://doi.org/10.2514/1.B36488.
[73] B. Esteves, C. Drag, A. Bourdon, A. Alvarez Laguna, P. Chabert, Experimental and numerical investigation of a gridded ion thruster running with different propellants (I, Xe, Kr, Ar), in: Proc. 37th Internat. Electric Propuls. Conf., Paper IEPC-2022-416, Cambridge, MA, USA, 2022.
[74] N. Fazio, S.B. Gabriel, I.O. Golosnoy, Alternative propellants for gridded ion engines, in: Proc. 37th Internat. Electric Propuls. Conf., 2022. Cambridge, MA, USA.
[75] D. Lauer, P. Valles, Ch Knorr, H. Leiter, Gridded ion engine standardized electric propulsion platforms – GIESEPP & GIESEPP-MP: results and outlook, in: Proc. 37th Internat. Electric Propuls. Conf., Paper IEPC-2022-280, Cambridge, MA, USA, 2022.
[76] F. Scholze, F. Pietag, C. Bundesmann, R. Woyciechowski, D. Spemann, M. Kreil, M. Kron, H. Adirim IonJet, Development of a cost-efficient gridded ion thruster propulsion system for smallsats, in: Proc. 37th Internat. Electric Propuls. Conf., Paper IEPC-2022-246, Cambridge, MA, USA, 2022.
[77] M. Ruiz, V. Gómez, P. Fajardo, J. Navarro, R. Albertoni, G. Dickeli, A. Vinci, S. Mazouffre, N. Hildebrand Hipatia, A project for the development of the Helicon Plasma Thruster and its associated technologies to intermediate-high TRLs, IAC-20-C4.5.12, in: 71st Internat. Astronaut. Congress (IAC), 2020. https://hal.science/hal-02995461.
[78] J. Navarro-Cavalle, M. Wijnen, P. Fajardo, E. Ahedo, V. Gomez, A. Gimenezk, M. Ruiz, Development and characterization of the helicon plasma thruster prototype HPT05M, in: 36th Internat. Electric Prop. Conf., paper IEPC-2019-596, 2019. http://electricrocket.org/2019/596.pdf.
[79] V. Gómez, M. Wijnen, J. Navarro-Cavallé, Direct thrust measurements of the HIPATIA system thruster, in: Proc. 37th Internat. Electric Propuls. Conf., Paper IEPC-2022-491, Cambridge, MA, USA, 2022.
[80] N.S. Mühlich, J. Gerger, B. Seifert, D. Krejci, F. Aumayr, Highly focused ion beam of a FEEP thruster generated with a compact electrostatic lens system, in: Proc. 37th Internat. Electric Propuls. Conf., IEPC-2022-189, Cambridge, MA, USA, 2022.
[81] S. Bathgate, M. Bilek, D. McKenzie, Electrodeless plasma thrusters for spacecraft: a review, Plasma Sci. Technol. 19 (2017) 083001.
[82] J. Skalden, M. Ehresmann, G. Herdrich, S. Fasoulas, Development of an AM Based Arcjet System for Deorbiting Constellation Satellites, 37th Internat. Electric Propuls. Conf., Cambridge, MA, USA, 2022. Paper IEPC-2022-578.

[83] B. Wollenhaupt, Q.H. Le, G. Herdrich, Overview of thermal arcjet thruster development, Aircraft Eng. Aero. Technol. 90 (2018) 280–301, https://doi.org/10.1108/AEAT-08-2016-0124.
[84] T. Ji, L. Wei, F. Wu, W. Jiang, W. Li, Y. Ding, H. Li, J. Geng, D. Yu, Recent progress in research on micro-cathode arc thrusters, European Phys. J. D. 74 (2020) 83, https://doi.org/10.1140/epjd/e2020-10032-9.
[85] T. Ji, L. Wei, Y. Wang, Y. Song, H. Cai, H. Li, Y. Ding, D. Yu, Influence of pulse frequency on discharge characteristics of micro-cathode arc thruster, Vacuum 196 (2022) 110748, https://doi.org/10.1016/j.vacuum.2021.110748.
[86] A. Anders, G.Y. Yushkov, Ion flux from vacuum arc cathode spots in the absence and presence of a magnetic field, J. Appl. Phys. 91 (2002) 4824, https://doi.org/10.1063/1.1459619.
[87] M. Galonska, R. Hollinger, I.A. Krinberg, P. Spaedtke, Influence of an axial magnetic field on the electron temperature in a vacuum arc plasma, IEEE Trans. Plasma Sci. 33 (2005) 1542–1547, https://doi.org/10.1109/TPS.2005.856504.
[88] G. Herdrich, M. Fertig, S. Löhle, Experimental simulation of high enthalpy planetary entries, Open J. Plasma Phys. 2 (2009) 150–164, https://doi.org/10.2174/1876534300902010150.
[89] K. Takahashi, Helicon-type radiofrequency plasma thrusters and magnetic plasma nozzles, Rev. Mod. Plasma Phys. 3 (2019) 3, https://doi.org/10.1007/s41614-019-0024-2.
[90] A.E. Vinci, S. Mazouffre, V. Gómez, P. Fajardo, J. Navarro-Cavallé, Laser-induced fluorescence spectroscopy on xenon atoms and ions in the magnetic nozzle of a Helicon plasma thruster, Plasma Sources Sci. Technol. 31 (2022) 095007, https://doi.org/10.1088/1361-6595/ac8db8.
[91] A.E. Vinci, Q. Delavière–Delion, S. Mazouffre, Electron thermodynamics along magnetic nozzle lines in a helicon plasma, J. Electric Propuls. 1 (2022) 4, https://doi.org/10.1007/s44205-022-00003-0.
[92] A.E. Vinci, S. Mazouffre, Plasma properties conditioned by the magnetic throat location in a helicon plasma device, J. Appl. Phys. 130 (2021) 183301, https://doi.org/10.1063/5.0069983.
[93] A.E. Vincia, S. Mazouffre, Effect of magnetic nozzle geometry on ion and electron properties, in: 73rd Internat. Astronautical Congress (IAC), Paper IAC–22–72147, Paris, France, 2022.
[94] Y.-A. Chan, G. Herdrich, Experimental verification of an electromagnetic nozzle on plasma confinement and acceleration, in: IEPC-2022-428, 37th Internat. Electric Propuls. Conf., MIT, Cambridge, MA USA, 2022.
[95] H. Böhrk, D. Petkow, G. Herdrich, M. Auweter-Kurtz, H. Kurtz, Arcjet stage investigation and inductive hydrogen heating in the TIHTUS Engine, Paper IEPC-2005-275, in: 29th Internat. Electric Propulsion Conference, Princeton University, 2005.
[96] D.B. Zolotukhin, K.P. Daniels, L. Brieda, M. Keidar, Onset of the magnetized arc and its effect on the momentum of a low-power two-stage pulsed magneto-plasma-dynamic thruster, Phys. Rev. E 102 (2020), https://doi.org/10.1103/PhysRevE.102.021203, 021203(R).
[97] D. Zolotukhin, K. Daniels, M. Keidar, Discharge characteristics of two-stage micro-cathode arc MPD thrusters with a permanent magnet and a pulsed magnetic field, J. Phys. D Appl. Phys. 54 (2021) 015201, https://doi.org/10.1088/1361-6463/abb7ba.
[98] O. Baranov, I. Levchenko, S. Xu, X.G. Wang, H.P. Zhou, K. Bazaka, Direct current arc plasma thrusters for space applications: basic physics, design and perspectives, Rev. Mod. Plasma Phys. 3 (2019) 7, https://doi.org/10.1007/s41614-019-0023-3.
[99] Z. Zhang, Z. Zhang, W. Yeong, L. Ling, X. Han, J. Zhou, H. Tang, J. Cao, Time-resolved investigation of the asymmetric plasma plume in a pulsed plasma thruster, J. Phys. D Appl. Phys. 53 (2020) 475201, https://doi.org/10.1088/1361-6463/abab2a.
[100] S.D. Baalrud, B. Scheiner, B.T. Yee, M.M. Hopkins, E. Barnat, Interaction of biased electrodes and plasmas: sheaths, double layers, and fireballs, Plasma Sources Sci. Technol. 29 (2020) 053001, https://doi.org/10.1088/1361-6595/ab8177.
[101] D.B. Zolotukhin, S. Hurley, M. Keidar, Anode ablation and performance improvement of microcathode arc thruster Plasma Sources, Sci. Technol. 28 (2019) 034001, https://doi.org/10.1088/1361-6595/ab01ec.
[102] J. Tian, W. Liu, W. Zhang, Y. Gao, L. Zhao, Micro-cathode arc thruster using segmented insulated anode with a slit for micro-satellite propulsion, Plasma Sources Sci. Technol. 29 (2020) 105005, https://doi.org/10.1088/1361-6595/abb41d.
[103] D.B. Zolotukhin, K.P. Daniels, S.R.P. Bandaru, M. Keidar, Magnetoplasmadynamic two-stage micro-cathode arc thruster for CubeSats Plasma Sources, Sci. Technol. 28 (2019) 105001, https://doi.org/10.1088/1361-6595/ab4170.
[104] D.B. Zolotukhin, M. Keidar, Optimization of discharge triggering in micro-cathode vacuum arc thruster for CubeSats, Plasma Sources Sci. Technol. 27 (2018) 074001, https://doi.org/10.1088/1361-6595/aacdb0.
[105] O. Baranov, U. Cvelbar, K. Bazaka, Concept of a magnetically enhanced vacuum arc thruster with controlled distribution of ion flux, IEEE Trans. Plasma Sci. 42 (2018) 304–310, https://doi.org/10.1109/TPS.2017.2778880.
[106] G. Herdrich, M. Fertig, S. Löhle, Experimental simulation of high enthalpy planetary entries, Open J. Plasma Phys. 2 (2009) 150–164, https://doi.org/10.2174/1876534300902010150.
[107] I. Kronhaus, M. Laterza, Y. Maor, Inline screw feeding vacuum arc thruster, Rev. Sci. Instrum. 88 (2017) 043505, https://doi.org/10.1063/1.4979706.
[108] I. Kronhaus, M. Laterza, A. Linossier, Experimental characterization of the inline-screw-feeding vacuum-arc-thruster operation, IEEE Trans. Plasma Sci. 46 (2018) 283–288, https://doi.org/10.1109/TPS.2017.2776839.
[109] S. Chowdhury, I. Kronhaus, Characterization of vacuum arc thruster performance in weak magnetic nozzle, Aerospace 7 (2020) 82, https://doi.org/10.3390/aerospace7060082.
[110] A. Sasoh, H. Kasuga, Y. Nakagawa, T. Matsuba, D. Ichihara, A. Iwakawa, Electrostatic-magnetic-hybrid thrust generation in central–cathode electrostatic thruster (CC–EST), Acta Astronaut. 152 (2018) 137–145, https://doi.org/10.1016/j.actaastro.2018.07.052.
[111] A. Sasoh, K. Mizutani, A. Iwakawa, Electrostatic/magnetic ion acceleration through a slowly diverging magnetic nozzle between a ring anode and an On-axis hollow cathode, AIP Adv. 7 (2017) 065204, https://doi.org/10.1063/1.4985380.
[112] D. Ichihara, A. Iwakawa, A. Sasoh, Effects of magnetic field profile near anode on ion acceleration characteristics of a diverging magnetic field electrostatic thruster, J. Appl. Phys. 122 (2017) 043302, https://doi.org/10.1063/1.4995286.
[113] D. Ichihara, A. Uchigashima, A. Iwakawa, A. Sasoh, Electrostatic ion acceleration across a diverging magnetic field, Appl. Phys. Lett. 109 (2016) 053901, https://doi.org/10.1063/1.4960363.
[114] K. Polzin, A. Martin, J. Little, C. Promislow, B. Jorns, J. Woods, State-of-the-Art and advancement paths for inductive pulsed plasma thrusters, Aerospace 7 (2020) 105, https://doi.org/10.3390/aerospace7080105.
[115] T. Furukawa, K. Takizawa, D. Kuwahara, S. Shinohara, Electrodeless plasma acceleration system using rotating magnetic field method, AIP Adv. 7 (2017) 115204, https://doi.org/10.1063/1.4998248.
[116] Y. Sun, I. Levchenko, J.W.M. Lim, L. Xu, S. Huang, Z. Zhang, F. Thio, G.-C. Potrivitu, M. Rohaizat, O. Cherkun, C.S. Chan, O. Baranov, K. Bazaka, S. Xu, Miniaturized rotating magnetic field driven plasma system: proof-of-concept experiments, Plasma Sources Sci. Technol. 30 (2021) 065003, https://doi.org/10.1088/1361-6595/ab9b34.
[117] T. Furukawa, S. Shinohara, D. Kuwahara, Electrodeless Plasma Propulsion with Electromagnetic Acceleration Effect by Using Rotating Magnetic Field Current Drive Method, 2020, https://doi.org/10.2514/6.2020-3630. Paper AIAA 2020-3630.
[118] T. Furukawa, K. Takizawa, D. Kuwahara, S. Shinohara, Study on electromagnetic plasma propulsion using rotating magnetic field acceleration scheme, Phys. Plasmas 24 (2017) 043505, https://doi.org/10.1063/1.4979677.
[119] H. Horita, D. Kuwahara, H. Akatsuka, S. Shinohara, Estimating electron temperature and density using improved collisional-radiative model in high-density RF argon plasma, AIP Adv. 11 (2021) 075226, https://doi.org/10.1063/5.0050215.
[120] T. Furukawa, D. Kuwahara, S. Shinohara, Spatial characteristics of rotating magnetic field (RMF) plasma acceleration method in open magnetic field configuration under partial RMF penetration, Phys. Plasmas 28 (2021) 073507, https://doi.org/10.1063/5.0035383.
[121] H. Liu, S. Shinohara, Y. Yu, M. Xu, P.F. Zheng, Z.H. Wang, S.B. Gong, H.J. Wang, Y.X. Zhu, L. Nie, R. Ke, Y.H. Chen, X.R. Duan, M.Y. Ye, A large-area planar helicon plasma source with a multi-ring antenna on Linear Experimental Advanced Device (LEAD), J. Instrum. 15 (2020) P11002, https://doi.org/10.1088/1748-0221/15/11/P11002.
[122] G. Becatti, D.M. Goebel, M. Zuin, Observation of rotating magnetohydrodynamic modes in the plume of a high-current hollow cathode, J. Appl. Phys. 129 (2021) 033304, https://doi.org/10.1063/5.0028566.
[123] D.M. Goebel, G. Becatti, I.G. Mikellides, A.L. Ortega, Plasma hollow cathodes, J. Appl. Phys. 130 (2021) 050902, https://doi.org/10.1063/5.0051228.
[124] B.A. Jorns, S.E. Cusson, Z. Brown, E. Dale, Non-classical electron transport in the cathode plume of a Hall effect thruster, Phys. Plasmas 27 (2020) 022311, https://doi.org/10.1063/1.5130680.
[125] M.S. McDonald, A.D. Gallimore, Rotating spoke instabilities in Hall thrusters, IEEE Trans. Plasma Sci. 39 (2011) 2952–2953, https://doi.org/10.1109/TPS.2011.2161343.
[126] D.M. Goebel, K.K. Jameson, I. Katz, I.G. Mikellides, Potential fluctuations and energetic ion production in hollow cathode discharges, Phys. Plasmas 14 (2007) 103508, https://doi.org/10.1063/1.2784460.
[127] J.A. Miller, Particle acceleration in impulsive solar flares, in: C.T. Russell, R. A. Mewaldt, T.T. Von Rosenvinge (Eds.), The Advanced Composition Explorer Mission, Springer, Dordrecht, 1998, https://doi.org/10.1007/978-94-011-4762-0_5.
[128] V. Petrosian, S. Liu, Stochastic acceleration of electrons and protons. I. Acceleration by parallel propagating waves, Astrophys. J. 610 (2004) 550, https://doi.org/10.1086/421486.
[129] J.F. Drake, P.A. Cassak, M.A. Shay, M. Swisdak, E. Quataert, A magnetic reconnecgtion mechanism for ion acceleration and abundance enhancements in impulsive flares, Astrophys. J. 700 (2009) L16–L20, https://doi.org/10.1088/0004-637X/700/1/L16.
[130] P. Dietz, W. Gärtner, Q. Koch, P.E. Köhler, Y. Teng, P.R. Schreiner, K. Holste, P. J. Klar, Molecular propellants for ion thrusters, Plasma Sources Sci. Technol. 28 (2019) 084001, https://doi.org/10.1088/1361-6595/ab2c6c.
[131] J. Yang, S. Jia, Z. Zhang, X. Zhang, T. Jin, L. Li, Y. Cai, J. Cai, Performance of a 4-cm iodine-fuelled radio frequency ion thruster, Plasma Sci. Technol. 22 (2020) 094006, https://doi.org/10.1088/2058-6272/ab891d.
[132] Y. Nakagawa, H. Koizumi, H. Kawahara, K. Komurasaki, Performance characterization of a miniature microwave discharge ion thruster operated with water, Acta Astronaut. 157 (2019) 294–299, https://doi.org/10.1016/j.actaastro.2018.12.031.
[133] D. Rafalskyi, J.M. Martínez, L. Habl, E.Z. Rossi, P. Proynov, A. Boré, T. Baret, A. Poyet, T. Lafleur, S. Dudin, A. Aanesland, In-orbit demonstration of an iodine electric propulsion system, Nature 599 (2021) 411–415, https://doi.org/10.1038/s41586-021-04015-y.

[134] I. Levchenko, K. Bazaka, Iodine powers low-cost engines for satellites, Nature 599 (2021) 373–374, https://doi.org/10.1038/d41586-021-03384-8.
[135] S. Serjeant, M. Elvis, G. Tinetti, The future of astronomy with small satellites, Nat. Astron. 4 (2020) 1031–1038.
[136] K.V. Mani, A. Cervone, F. Topputo, Combined chemical-electric propulsion for a stand-alone Mars CubeSat, J. Spacecraft Rockets 56 (2019) 1816–1830.
[137] D. Tsifakis, C. Charles, R. Boswell. Naphthalene as a Cubesat Cold Gas Thruster Propellant. Front. Phys. 8, 389, 2020.
[138] J. Szabo, M. Robin, V. Hruby, Bismuth vapor Hall effect thruster performance and plume experiments, in: 35th Internat. Electric Prop. Conf., Atlanta, Georgia, USA, 2017. Paper IEPC-2017-25.
[139] Y. Ou, J. Wu, Y. Zhang, J. Li, Comparative study of plume characteristics of polymeric propellants filled with different oxides for laser-electric hybrid thruster, Opt Laser. Technol. 147 (2022) 107609, https://doi.org/10.1016/j.optlastec.2021.107609.
[140] D.J. Förster, B. Jäggi, A. Michalowski, B. Neuenschwander, Review on experimental and theoretical investigations of ultra-short pulsed laser ablation of metals with burst pulses, Materials 14 (2021) 3331. https://doi.org/10.3390/ma14123331.
[141] M. Krishnan, K. Velas, S. Leemans, Metal plasma thruster for small satellites, J. Propul. Power 36 (2020) 4, https://doi.org/10.2514/1.B37603.
[142] Y. Ou, J. Wu, Y. Zhang, J. Li, Y. Zhao, Plume characteristics of polymeric material doped with different metal particles under pulsed laser irradiation, Opt Laser. Technol. 152 (2022) 108132, https://doi.org/10.1016/j.optlastec.2022.108132.
[143] O. Yang, J. Wu, Y. Zhang, J. Li, Modeling the laser-polymer interaction of laser propulsion systems considering progressive surface removal, thermal decomposition and non-Fourier effect, Acta Astronaut. 186 (2021) 319–328, https://doi.org/10.1016/j.actaastro.2021.05.042.
[144] R. Gaudenzi, D. Stefani, S.J. Cartamil-Bueno, Light-induced propulsion of graphene-on-grid sails in microgravity, Acta Astronaut. 174 (2020) 204–210, https://doi.org/10.1016/j.actaastro.2020.03.030.
[145] T. Kamei, M. Matsui, K. Mori, Feasibility study of a laser launch system for picosatellites and nanosatellites in low-earth orbits, Acta Astronaut. 176 (2020) 124–130, https://doi.org/10.1016/j.actaastro.2020.06.014.
[146] M.A. Hopkins, L.B. King, Performance comparison between a magnesium- and xenon-fueled 2 kilowatt Hall thruster, J. Propul. Power 32 (2016) 1015–1021, https://doi.org/10.2514/1.B35731.
[147] J.R. Brophy, J.E. Polk, D.M. Goebel, Development of a 50,000-s, lithium-fueled, gridded ion thruster, in: Proc. 35th Internat. Electric Prop. Conf., Atlanta, GA, USA, 2017.
[148] H. Kamhawi, T. Haag, G. Benavides, T. Hickman, T. Smith, G. Williams, J. L. Myers, K.A. Polzin, J. Dankanich, L. Byrne, et al., Overview of iodine propellant hall thruster development activities at NASA Glenn research center, in: Proc. 52nd AIAA/SAE/ASEE Joint Prop. Conf., Salt Lake City, UT, USA, 2016.
[149] Condensable Propellant Hall Thrusters. http://aerospace.mtu.edu/research/condensable-propellant-hall-thrusters (Accessed January **2022**).
[150] Space micropropulsion website, www.micropropulsion.org (Accessed April 2022).
[151] Busek company, Hall thrusters. https://www.busek.com/hall-thrusters (Accessed January 2022).
[152] Y. Ou, Y. Zhang, J. Wu, J. Li, S. Tan, Y. Zhao, Comparative study of PTFE filled different dopants as propellants for laser-electric hybrid thruster, Acta Astronaut. 183 (2021) 199–210, https://doi.org/10.1016/j.actaastro.2021.03.018.
[153] Y. Ou, J. Wu, Y. Zhang, J. Li, Effects of carbon, graphite, and graphene as propellant dopants in a laser-electric hybrid acceleration system, Opt Laser. Technol. 151 (2022) 108007, https://doi.org/10.1016/j.optlastec.2022.108007.
[154] S. Shinohara, D. Kuwahara, Y. Ishigami, H. Horita, S. Nakanishi, Extremely small-diameter, high-density, radio frequency, plasma sources and central gas feeding for next-generation electrodeless plasma thrusters, Rev. Sci. Instrum. 91 (2020) 073507, https://doi.org/10.1063/5.0003387.
[155] G. Herdrich, M. Auweter-Kurtz, H. Kurtz, E. Schreiber, Investigation of the inductively heated plasmagenerator IPG3 using Injection rings of different geometries, in: 21st AIAA Adv. Measurement Technology and Ground Testing Conference, Paper AIAA-2000-2445, Juni, Denver, CO, 2000.
[156] J. Simmonds, Y. Raitses, Ion acceleration in a wall-less Hall thruster, J. Appl. Phys. 130 (2021) 093302, https://doi.org/10.1063/5.0062607.
[157] Y. Ding, B. Jia, Y. Xu, L. Wei, H. Su, P. Li, H. Sun, W. Peng, Y. Cao, D. Yu, Effect of vortex inlet mode on low-power cylindrical Hall thruster, Phys. Plasmas 24 (2017) 080703, https://doi.org/10.1063/1.4986007.
[158] G. Xia, H. Li, Y. Ding, L. Wei, S. Chen, D. Yu, Performance optimization of a krypton Hall thruster with a rotating propellant supply, Acta Astronaut. 171 (2020) 290–299, https://doi.org/10.1016/j.actaastro.2020.03.021.
[159] G. Xia, H. Lia, X. Zhu, Z. Ning, S. Chen, D. Yu, C. Zhou, Effects of rotating supply mode on the ionization parameters of a krypton Hall thruster, Vacuum 181 (2020) 109664, https://doi.org/10.1016/j.vacuum.2020.109664.
[160] O. Hamo, I. Kronhaus, Experimental and numerical characterization of the narrow channel Hall thruster discharge, J. Appl. Phys. 130 (2021) 223301, https://doi.org/10.1063/5.0067264.
[161] Y. Wang, L. Ren, W. Ding, A. Sun, Plasma plume evolution of a capillary discharge based pulsed plasma thruster: an optical diagnosis study, Phys. Plasmas 28 (2021) 123509, https://doi.org/10.1063/5.0056491.
[162] N. Gondol, M. Tajmar, Design of a Hollow Cathode Thruster: Concepts, Parameter Study and Initial Test Results, CEAS Space J, 2021, https://doi.org/10.1007/s12567-021-00369-1.
[163] I. Kronhaus, A. Warshavsky, Narrow Channel Hall Thruster, Israel patent publication, 2017 256341. WO 2019/1163 71A1 (June **2019**).
[164] I. Kronhaus, A. Linossier, Experimental characterization of the narrow channel Hall thruster, Plasma Sources Sci. Technol. 27 (2018) 124005, https://doi.org/10.1088/1361-6595/aaec65.
[165] I. Kronhaus, O. Hamo, 2D particle-in-cell channel simulation of the narrow channel Hall thruster, in: Proc. 36th Internat. Electric Propul. Conf., paper IEPC-2019-642, Vienna, Austria, 2019. http://electricrocket.org/2019/642.pdf.
[166] Y.N. Wang, W.D. Ding, L. Cheng, J.Q. Yan, Z.C. Li, J.C. Wang, Y.S. Wang, IEEE Trans. Plasma Sci. 45 (2017) 2715–2724, https://doi.org/10.1109/TPS.2017.2738330.
[167] A. Quraishi, I. Kronhaus, A. Reeh, U. Probst, Mode transition in capillary capacitively radio frequency thruster, IEEE Trans. Plasma Sci. 49 (2021) 635–647, https://doi.org/10.1109/TPS.2020.3047011.
[168] A. Quraishi, I. Kronhaus, Modelling of capillary capacitively coupled radio frequency thruster, J. Phys. D Appl. Phys. 54 (2021) 425201, https://doi.org/10.1088/1361-6463/ac16a5.
[169] R.L. Forward, Negative matter propulsion, J. Propulsion 6 (2012) 28, https://doi.org/10.2514/3.23219.
[170] M.A. Khamehchi, K. Hossain, M.E. Mossman, Y. Zhang, Th Busch, M. Mc Forbes, P. Engels, Negative-mass hydrodynamics in a spin-orbit–coupled Bose–Einstein condensate, Phys. Rev. Lett. 118 (2017) 155301, https://doi.org/10.1103/PhysRevLett.118.155301.
[171] A. Griffin, The Independent, Scientists Observe Liquid with 'negative Mass', Which Turns Physics Completely Upside Down, 2017. (Accessed 15 December 2020).
[172] N. Mortillaro, CBC News, Scientists Create Fluid that Seems to Defy Physics: 'Negative Mass' Reacts Opposite to Any Known Physical Property We Know, 2017. https://www.cbc.ca/news/science/fluid-negative-mass-1.4073937. (Accessed 11 December 2020).
[173] R. Hofer, High-specific impulse operation of the BPT-4000 hall thruster for NASA science missions, in: Proceedings of the 46th AIAA/ASME/SAE/ASEE Joint Propulsion Conference and Exhibit, Nashville, Tennessee, USA, 2010.
[174] J.W.M. Lim, S.Y. Huang, L. Xu, J.S. Yee, R.Z. Sim, Z.L. Zhang, I. Levchenko, S. Xu, Automated integrated robotic systems for diagnostics and test of electric and micropropulsion thrusters, IEEE Trans. Plasma Sci. 46 (2018) 345–353, https://doi.org/10.1109/TPS.2018.2795023.
[175] M.G. Allen, J. Eckels, M.P. Byrne, A.A. Gorodetsky, B.A. Jorns, Application of Optimal Experimental Design to Characterize Pressure Related Facility Effects in a Hall Thruster, 2022. Paper IEPC-2022- ####, Boston, MA.
[176] A. Thuppul, P.L. Wright, A.L. Collins, J.K. Ziemer, R.E. Wirz, Lifetime considerations for electrospray thrusters, Aerospace 7 (2020) 108, https://doi.org/10.3390/aerospace7080108.
[177] N.P. Brown, M.L.R. Walker, Review of plasma-induced Hall thruster erosion, Appl. Sci. 10 (2020) 3–7, https://doi.org/10.3390/app10113775.
[178] D. O'Reilly, G. Herdrich, D.F. Kavanagh, Electric propulsion methods for small satellites: a review, Aerospace 8 (2021) 22, https://doi.org/10.3390/aerospace8010022.
[179] D. Krejci, P. Lozano, Space propulsion technology for small spacecraft, Proc. IEEE 106 (2018) 362–378, https://doi.org/10.1109/JPROC.2017.2778747.
[180] G. Becatti, W.R. Conversano, D.M. Goebel, Demonstration of 25,000 ignitions on a proto-flight compact heaterless lanthanum hexaboride hollow cathode, Acta Astronaut. 178 (2020) 181–191, https://doi.org/10.1016/j.actaastro.2020.09.013.
[181] E.Y. Choueiri, R. Spector, Coherent ion acceleration using two electrostatic waves, 16-19 July, in: 36th AIAA/ASME/SAE/ASEE Joint Prop. Conf. Exhibit, Paper AIAA-2000-3759, Huntsville, AL, USA, 2000, https://doi.org/10.2514/6.2000-3759.
[182] B. Jorns, E.Y. Choueiri, Stochastic ion acceleration by beating electrostatic waves, Phys. Rev. E 87 (2013) 013107, https://doi.org/10.1103/PhysRevE.87.013107.
[183] R. Spektor, E.Y. Choueiri, Ion acceleration by beating electrostatic waves: domain of allowed acceleration, Phys. Rev. E 69 (2004) 046402, https://doi.org/10.1103/PhysRevE.69.046402.
[184] H. Kang, J. Lee, K.-T. Kim, Y.-H. Song, D.H. Lee, Conceptual demonstration of Martian atmosphere-breathing electrical supersonic thruster with CO2-based rotating gliding arc, Acta Astronaut. 200 (2022) 196–200, https://doi.org/10.1016/j.actaastro.2022.07.058.
[185] V. Saini, R. Ganesh, Double layer formation and thrust generation in an expanding plasma using 1D-3V PIC simulation. Double layer formation and thrust generation in an expanding plasma using 1D-3V PIC simulation, Phys. Plasmas 27 (2020) 093505, https://doi.org/10.1063/5.0004335.
[186] Y. Zhang, C. Charles, R. Boswell, Transport of ion beam in an annular magnetically expanding helicon double layer thruster, Phys. Plasmas 21 (2014) 063511, https://doi.org/10.1063/1.4885350.
[187] T. Harle, S.J. Pottinger, V.J. Lappas, Helicon double layer thruster operation in a low magnetic field mode, Plasma Sources Sci. Technol. 22 (2013) 015015, https://doi.org/10.1088/0963-0252/22/1/015015.
[188] K. Takahashi, C. Charles, R. Boswell, A. Ando, Effect of magnetic and physical nozzles on plasma thruster performance, Plasma Sources Sci. Technol. 23 (2014) 044004, https://doi.org/10.1088/0963-0252/23/4/044004.
[189] F. Boni, V. Désangles, J. Jarrige, Experimental characterization of thrust production mechanisms in a magnetic nozzle ECR thruster, J. Electric Propuls. 1 (2022) 33, https://doi.org/10.1007/s44205-022-00034-7.
[190] S. Shinohara, T. Tanikawa, T. Hada, I. Funaki, H. Nishida, T. Matsuoka, F. Otsuka, K.P. Shamrai, T.S. Rudenko, T. Nakamura, A. Mishio, H. Ishii, N. Teshigahara, H. Fujitsuka, S. Waseda, High-density helicon plasma sources: basics and application to electrodeless electric propulsion, Fusion Sci. Technol. 63 (2013) 164–167, https://doi.org/10.13182/FST13-A16896.

[191] F. Otsuka, T. Hada, S. Shinohara, T. Tanikawa, T. Matsuoka, Numerical modeling of electrodeless electric thruster by ion cyclotron resonance/ponderomotive acceleration, Plasma Fusion Res. 8 (2013) 2406067, https://doi.org/10.1585/pfr.8.2406067.
[192] R. Nomura, N. Ohnishi, H. Nishida, PIC simulation of electrodeless plasma thruster with rotating electric field. 28th international symposium on rarefied gas dynamics, AIP Conf. Proc. 1501 (2012) 1431–1436, https://doi.org/10.1063/1.4769707.
[193] T. Nakamura, K. Yokoi, H. Nishida, S. Shinohara, I. Funaki, T. Matsuoka, T. Tanikawa, T. Hada, K.P. Shamrai, T.S. Rudenko, Experimental investigation of plasma acceleration by rotating electric field for electrodeless plasma thruster, in: The 32nd International Electric Propulsion Conference (IEPC), Wiesbaden, Germany, September 11-15, 2011, pp. 1–10.
[194] J. Wu, P. Zheng, Y. Zhang, H. Tang, Recent development of intake devices for atmosphere-breathing electric propulsion system, Prog. Aero. Sci. 133 (2022) 100848, https://doi.org/10.1016/j.paerosci.2022.100848.
[195] N.H. Crisp, P.C.E. Roberts, S. Livadiotti, V.T.A. Oiko, S. Edmondson, S.J. Haigh, C. Huyton, L.A. Sinpetru, K.L. Smith, S.D. Worrall, J. Becedas, R.M. Domínguez, D. González, V. Hanessian, A. Mølgaard, J. Nielsen, M. Bisgaard, Y.A. Chan, S. Fasoulas, G.H. Herdrich, F. Romano, C. Traub, D. García-Almiñana, S. Rodríguez-Donaire, M. Sureda, D. Kataria, R. Outlaw, B. Belkouchi, A. Conte, J. S. Perez, R. Villain, B. Heißerer, A. Schwalber, The benefits of very low earth orbit for earth observation missions, Prog. Aero. Sci. 117 (2020) 100619.
[196] F. Romano, Y.A. Chan, G. Herdrich, C. Traub, S. Fasoulas, P.C.E. Roberts, K. Smith, S. Edmondson, S. Haigh, N.H. Crisp, V.T.A. Oiko, S.D. Worrall, S. Livadiotti, C. Huyton, L.A. Sinpetru, A. Straker, J. Becedas, R.M. Domínguez, D. González, V. Cañas, V. Sulliotti-Linner, V. Hanessian, A. Mølgaard, J. Nielsen, M. Bisgaard, D. Garcia-Almiñana, S. Rodriguez-Donaire, M. Sureda, D. Kataria, R. Outlaw, R. Villain, J.S. Perez, A. Conte, B. Belkouchi, A. Schwalber, B. Heißerer, RF helicon-based inductive plasma thruster (IPT) design for an atmosphere-breathing electric propulsion system (ABEP), Acta Astronaut. 176 (2020) 476–483, https://doi.org/10.1016/j.actaastro.2020.07.008.
[197] P. Zheng, J. Wu, Y. Zhang, B. Wu, A comprehensive review of atmosphere-breathing electric propulsion systems, Int. J. Aerospace Eng. 2020 (2020) 1–21.
[198] F. Romano, Y.-A. Chan, G. Herdrich, C. Traub, S. Fasoulas, P.C.E. Roberts, K. Smith, S. Edmondson, S. Haigh, N.H. Crisp, V.T.A. Oiko, S.D. Worrall, S. Livadiotti, C. Huyton, L.A. Sinpetru, A. Straker, J. Becedas, R.M. Domínguez, D. González, V. Cañas, V. Sulliotti-Linner, V. Hanessian, A. Mølgaard, J. Nielsen, M. Bisgaard, D. Garcia-Almiñana, S. Rodriguez-Donaire, M. Sureda, D. Kataria, R. Outlaw, R. Villain, J.S. Perez, A. Conte, B. Belkouchi, A. Schwalber, B. Heißerer, RF helicon-based inductive plasma thruster (IPT) design for an atmosphere-breathing electric propulsion system (ABEP), Acta Astronaut. 176 (2020) 476–483, https://doi.org/10.1016/j.actaastro.2020.07.008.
[199] S.G. Bilen, C.L. Johnson, B.M. Wiegmann, L. Alexander, B.E. Gilchrist, R.P. Hoyt, C.H. Elder, K.P. Fuhrhop, M. Scadera, N. Stone, The PROPEL electrodynamic tether demonstration mission, in: AIAA SPACE 2012 Conference and Exposition, Paper AIAA 2012-5293, 2012, https://doi.org/10.2514/6.2012-5293.
[200] H. Fujii, T. Watanabe, H. Sahara, H. Kojima, S. Takehara, Y. Yamagiwa, S. Sasaki, T. Abe, K. Tanaka, K. Oyama, et al., Space demonstration of bare electrodynamic tape-tether technology on the sounding rocket S520-25, in: AIAA Guidance, Navigation, and Control Conference, Paper AIAA 2011-6503,, Portland, Oregon, 2011, https://doi.org/10.2514/6.2011-6503.
[201] R.P. Hoyt, Propulsion and power harvesting performance of electrodynamic tethers, in: AIAA Space 2011 Conf, Paper AIAA 2011-7321, Long Beach, CA, 2011, https://doi.org/10.2514/6.2011-7321.
[202] I. Katz, J.R. Lilley Jr., A. Greb, J.E. McCoy, J. Galofaro, D.C. Ferguson, Plasma turbulence enhanced current collection: results from the plasma motor generator electrodynamic tether flight, J. Geophys. Res. Space Phys. 100 (1995) 1687–1690, https://doi.org/10.1029/94JA03142.
[203] M.J. Gerver, D.E. Hastings, M.R. Oberhardt, Theory of plasma contactors in ground-based experiments and low earth orbit, J. Spacecraft Rockets 27 (1990) 391, https://doi.org/10.2514/3.26156.
[204] I. Levchenko, S. Xu, G. Teel, D. Mariotti, M.L.R. Walker, M. Keidar, Recent progress and perspectives of space electric propulsion systems based on smart nanomaterials, Nat. Commun. 9 (2018) 879, https://doi.org/10.1038/s41467-017-02269-7.
[205] F. Romei, A.N. Grubišić, Validation of an additively manufactured resistojet through experimental and computational analysis, Acta Astronaut. 167 (2020) 14–22, https://doi.org/10.1016/j.actaastro.2019.10.046.
[206] M.Z. Naser, A.I. Chehab, Materials and design concepts for space-resilient structures, Prog. Aero. Sci. 98 (2018) 74–90, https://doi.org/10.1016/j.paerosci.2018.03.004.
[207] I. Levchenko, S. Xu, O. Cherkun, O. Baranov, K. Bazaka, Plasma meets metamatertials: three ways to advance space micropropulsion systems, Adv. Phys. X 6 (2021) 1834452, https://doi.org/10.1080/23746149.2020.1834452.
[208] J.U. Surjadi, L. Gao, H. Du, X. Li, X. Xiong, N. Xuanlai, Mechanical metamaterials and their engineering applications, Adv. Eng. Mater. 21 (2019) 1800864, https://doi.org/10.1002/adem.201800864.
[209] R. Previdi, I. Levchenko, M. Arnold, M. Gali, K. Bazaka, S. Xu, K. Ostrikov, K. Bray, D. Jin, J. Fang, Plasmonic platform based on nanoporous alumina membranes: order control via self-assembly, J. Mater. Chem. 7 (2019) 9565–9577, https://doi.org/10.1039/C8TA11374B.
[210] I. Levchenko, K. Bazaka, T. Belmonte, M. Keidar, S. Xu, Advanced materials for next generation spacecraft, Adv. Mater. 30 (2018) 1802201, https://doi.org/10.1002/adma.201802201.
[211] I. Levchenko, K. Bazaka, M. Keidar, S. Xu, J. FangJ, Hierarchical multicomponent inorganic metamaterials: intrinsically driven self-assembly at the nanoscale, Adv. Mater. 30 (2018) 1702226, https://doi.org/10.1002/adma.201702226.
[212] F. Romei, A. Grubisic, Numerical study of a novel monolithic heat exchanger for electrothermal space propulsion, Acta Astronaut. 159 (2019) 8–16, https://doi.org/10.1016/j.actaastro.2019.03.025.
[213] I. Levchenko, I.I. Beilis, M. Keidar, Nanoscaled metamaterial as an advanced heat pump and cooling media, Adv. Mater. Technol. 1 (2016) 1600008, https://doi.org/10.1002/admt.201600008.
[214] H. Seppänen, T. Rauhala, S. Kiprich, J. Ukkonen, M. Simonsson, R. Kurppa, P. Janhunen, E. Hæggström, One kilometer (1 km) electric solar wind sail tether produce, Rev. Sci. Instrum. 84 (2013) 095102, https://doi.org/10.1063/1.4819795.
[215] N. Singhal, I. Levchenko, S. Huang, L. Xu, G.-C. Potrivitu, O. Cherkun, J. Fang, K. Bazaka, S. Xu, 3D-Printed multilayered reinforced material system for gas supply in cubesats and small satellites, Adv. Eng. Mater. 21 (2019) 1900401, https://doi.org/10.1002/adem.201900401.
[216] D.V.M. Maximo, L.F. Velasquez-García, Additively manufactured electrohydrodynamic ionic liquid pure-ion sources for nanosatellite propulsion, Addit. Manuf. 36 (2020) 101719, https://doi.org/10.1016/j.addma.2020.101719.
[217] F. Romei, A.N. Grubišić, D. Gibbon, Manufacturing of a high-temperature resistojet heat exchanger by selective laser melting, Acta Astronaut. 138 (2017) 356–368, https://doi.org/10.1016/J.ACTAASTRO.2017.05.020.
[218] I. Levchenko, O. Baranov, M. Keidar, C. Riccardi, H.E. Roman, S. Xu, Additive technologies and materials for the next-generation CubeSats and small satellites, Adv. Functional Mater. 34 (2024) 2407602. https://doi.org/10.1002/adfm.202407602.
[219] M.I.A.A. Maksoud, R.A. Fahim, A.E. Shalan, M.A. Elkodous, S.O. Olojede, A. I. Osman, C. Farrell, A.H. Al-Muhtaseb, A.S. Awed, A.H. Ashour, D.W. Rooney, Advanced materials and technologies for supercapacitors used in energy conversion and storage: a review, Environ. Chem. Lett. 19 (2021) 375–439, https://doi.org/10.1007/s10311-020-01075-w.
[220] R. Tamilselvi, M. Ramesh, G.S. Lekshmi, O. Bazaka, I. Levchenko, K. Bazaka, M. Mandhakini, Graphene oxide–Based supercapacitors from agricultural wastes: a step to mass production of highly efficient electrodes for electrical transportation systems, Renew. Energy 151 (2020) 731–739, https://doi.org/10.1016/j.renene.2019.11.072.
[221] S. Yuan, W. Fan, Y. Jin, D. Wang, T. Liu, Free-standing flexible graphene-based aerogel film with high energy density as an electrode for supercapacitors, Nano Mater. Sci. 3 (2020) 68–74, https://doi.org/10.1016/j.nanoms.2020.03.003.
[222] A. Kandasamy, T. Ramasamy, A. Samrin, P. Narayanasamy, R. Mohan, O. Bazaka, I. Levchenko, K. Bazaka, M. Mohandas, Hierarchical doped gelatin-derived carbon aerogels: three levels of porosity for advanced supercapacitors, Nanomaterials 10 (2020) 1178, https://doi.org/10.3390/nano10061178.
[223] M. Yaseen, M.A.K. Khattak, M. Humayun, M. Usman, S.S. Shah, S. Bibi, B.S. U. Hasnain, S.M. Ahmad, A. Khan, N. Shah, A.A. Tahir, H. Ullah, A review of supercapacitors: materials design, modification, and applications, Energies 14 (2021) 7779, https://doi.org/10.3390/en14227779.
[224] I. Levchenko, S. Xu, O. Baranov, O. Bazaka, E.P. Ivanova, K. Bazaka, Plasma and polymers: recent progress and trends, Molecules 26 (2021) 4091, https://doi.org/10.3390/molecules26134091.
[225] C. Piferi, K. Bazaka, D.L. D'Aversa, R. Di Girolamo, C. De Rosa, H.E. Roman, C. Riccardi, I. Levchenko, Hydrophilicity and hydrophobicity control of plasma-treated surfaces via fractal parameters, Adv. Mater. Interfac. 8 (2021) 2100724, https://doi.org/10.1002/admi.202100724.